

TECHNICAL UNIVERSITY OF CRETE  
ELECTRONIC AND COMPUTER ENGINEERING DEPARTMENT  
TELECOMMUNICATIONS DIVISION



# Distributed Zero-Feedback Beamforming for Emergency Radio

by

Alexandris Konstantinos

A THESIS SUBMITTED IN PARTIAL FULFILLMENT OF  
THE REQUIREMENTS FOR THE DIPLOMA DEGREE OF

ELECTRONIC AND COMPUTER ENGINEERING

September 2012

THESIS COMMITTEE

Assistant Professor Aggelos Bletsas, *Thesis Supervisor*

Assistant Professor George N. Karystinos

Professor Athanasios P. Liavas



# Abstract

Ubiquitous wireless sensor networks (WSNs) have emerged as an important research theme in wireless communication and networking. Distributed transmit beamforming, applied in WSNs, exploits cooperative transmission from two or more distributed transceivers, such that the phases of their transmitted signals align and offer a constructive gain towards the intended destination receiver. Several distributed beamforming techniques for boosting signal power are based on channel state information (CSI) or feedback (from the receiver) availability at the distributed transmitters, as well as some ability to access the transmitter radio module for carrier phase adjustments. Contrary to prior art, this thesis considers no CSI availability, no receiver-based feedback and low-cost commodity, off-the-self WSN radios. *Two concrete non-coherent receivers* for zero-feedback beamforming are presented. The first near-optimal non-coherent receiver exploits zero-feedback (i.e. blind), constructive, distributed signal alignment after repetitive transmission, while the second one is based on maximum likelihood (ML) and exploits diversity. Analysis and simulation bit-error-rate (BER) results are demonstrated. The two proposed receivers could alleviate network partitioning problems and could be easily implemented with low-cost commodity radio hardware.



# Acknowledgements

I would like to take some time here and thank the people who made the completion of this work possible. First of all, my parents, without whom my entire studies would not have been possible. I would also like to thank all my friends for encouraging and supporting me all these years. Next, I need to thank all the people who create such a good atmosphere in the lab. I also need to acknowledge my thesis supervisor, Assistant Professor Aggelos Bletsas, for all his guidance, support and patience. Finally, I would like to thank my committee members who graciously agreed to serve on my committee.



# Table of Contents

<b>Table of Contents</b> . . . . .	7
<b>List of Figures</b> . . . . .	9
<b>List of Tables</b> . . . . .	11
<b>List of Abbreviations</b> . . . . .	13
<b>Preface</b> . . . . .	15
<b>1 Introduction</b> . . . . .	17
1.1 Motivation . . . . .	17
1.2 Related Work . . . . .	17
1.3 Thesis outline . . . . .	18
<b>2 Beamforming using repetition coding</b> . . . . .	21
2.1 Signal model . . . . .	21
2.2 Alignment probability of M signals . . . . .	23
2.2.1 Alignment event . . . . .	23
2.2.2 Alignment probability . . . . .	25
2.3 Protocol . . . . .	26
2.4 Non-coherent detector . . . . .	27
2.5 Simulation . . . . .	31
<b>3 Beamforming using interleaving</b> . . . . .	35
3.1 Protocol . . . . .	35
3.2 Coherent Detection . . . . .	40
3.2.1 ML coherent detector . . . . .	40

---

3.2.2	BER performance analysis . . . . .	41
3.2.3	Diversity . . . . .	43
3.3	Non-Coherent Detection . . . . .	45
3.3.1	ML non-coherent detector . . . . .	45
3.3.2	BER performance analysis . . . . .	47
3.4	Single symbol case analysis . . . . .	48
3.5	Alamouti reception scheme . . . . .	49
3.6	Simulation . . . . .	50
<b>4</b>	<b>Unitary Space-Time Constellations . . . . .</b>	<b>55</b>
4.1	System model . . . . .	55
4.2	Non-coherent detector . . . . .	56
4.3	Systematic design of unitary space-time constellations . . . . .	57
4.4	Simulation . . . . .	58
<b>5</b>	<b>Conclusions and future work . . . . .</b>	<b>61</b>
5.1	Conclusions . . . . .	61
5.2	Future work . . . . .	61
<b>Appendix A</b>	<b>. . . . .</b>	<b>63</b>
A.1	Proper complex Gaussian random vectors . . . . .	63
A.2	Gamma distribution . . . . .	63
<b>Bibliography</b>	<b>. . . . .</b>	<b>65</b>

# List of Figures

1.1	Firefighter scenario . . . . .	18
2.1	System model . . . . .	22
2.2	Alignment . . . . .	24
2.3	Alignment probability vs time (symbol number $n$ ) . . . . .	26
2.4	Repetition coding . . . . .	27
2.5	Independent random implementation of $ y_l ^2$ for the two hypotheses (SNR (dB) per transmitter antenna = 0) . . . . .	30
2.6	Independent random implementation of $ y_l ^2$ for the two hypotheses (SNR (dB) per transmitter antenna = 18) . . . . .	31
2.7	Proper $k$ parameter selection for repetition coding . . . . .	32
2.8	Simulation BER performance using proper $k$ parameter with different number of transmitters . . . . .	33
2.9	Simulation BER performance in different $L$ time intervals . . . . .	34
3.1	Interleaving . . . . .	36
3.2	Alamouti reception scheme . . . . .	49
3.3	Simulation and analysis BER performance for symbol case with different number of transmitters . . . . .	51
3.4	Simulation and analysis BER performance for interleaving transmission in different phases . . . . .	52
3.5	Simulation and analysis BER performance for interleaving transmission with different number of transmitters . . . . .	53
4.1	Simulation BER performance using USTM for $M = 2$ , $T = 8$ and $R = 1$ bit/symbol . . . . .	59



## List of Tables



## List of Abbreviations

BER	Bit Error Rate
CFO	Carrier Frequency Offset
CSI	Channel State Information
CWGN	Complex White Gaussian Noise
DFT	Discrete Fourier Transform
MAP	Maximum-a-Posteriori probability
ML	Maximum Likelihood
pdf	probability density function
ppm	parts per million
rv	random variable
SNR	Signal to Noise Ratio
USTC	Unitary Space-Time Constellation
USTM	Unitary Space-Time Modulation
WSN	Wireless Sensor Network



# Preface

Definitions, theorems, lemmas corollaries and examples share the same index within each chapter. The symbol  $\square$  stands for the end of proof of theorem, or lemma.

$x$	a variable
$\mathbf{x}$	a vector
$\mathbf{A}$	a matrix
$\mathbf{A}^T$	transpose of $\mathbf{A}$
$\mathbf{A}^\dagger$	conjugate transpose of $\mathbf{A}$
$\mathbf{I}_N$	$N \times N$ identity matrix
$ x $	the absolute value of a real or complex number
$\ \mathbf{x}\ _2$	the $\mathcal{L}_2$ norm of a vector $\mathbf{x}$
$\ \mathbf{A}\ $	the Frobenius norm of a matrix $\mathbf{A}$
$\mathbb{N}$	the set of natural numbers
$\mathbb{Z}$	the set of integer numbers
$\mathbb{C}$	the set of complex numbers
$\text{tr}\{\cdot\}$	the trace operator
$\text{vec}(\cdot)$	the vec operator
$\Re(\cdot)$	the real part of a complex number
$Q(\cdot)$	the Q-function
$\mathcal{O}(\cdot)$	the order of magnitude
$\mathcal{CN}(\boldsymbol{\mu}, \boldsymbol{\Sigma})$	denotes the distribution of a $N$ -dimensional proper complex Gaussian random vector with mean vector $\boldsymbol{\mu}$ and covariance matrix $\boldsymbol{\Sigma}$ <sup>1</sup>
$\mathcal{G}(k, \theta)$	denotes the Gamma distribution with parameters $k, \theta$ <sup>1</sup>

---

<sup>1</sup>The closed form of the distributions is placed in Appendix A.



# Chapter 1

## Introduction

### 1.1 Motivation

Distributed transmit beamforming (or simply distributed beamforming) is a form of cooperative communication in which two or more distributed terminals simultaneously transmit a common message, such that the phases of their transmissions align and offer a constructive gain towards the intended destination receiver. Many distributed beamforming designs have been proposed to boost the power of the transmitted signal and improve connectivity in resource-constrained networks. Another benefit of distributed beamforming is the high directivity offered when the network is designed to operate as a virtual antenna array. Finally, distributed beamforming may also provide benefits in terms of security and interference reduction, since less power is consumed towards unintended directions.

### 1.2 Related Work

There is vast literature on numerous practical challenges of distributed beamforming design. Beamforming setups make use of powerful optimization tools (e.g. [1], [2]) that require some type of prior knowledge, e.g. in the form of channel state information (CSI) or its second order statistics, in order to minimize the total transmit power and maximize the received signal-to-noise ratio (SNR). Beyond the battery-operated sensors, the low-complexity radios and the low-cost isotropic antennas in WSNs, where a great amount of research has been conducted in order to reduce power consumption, there is another great challenge of distributed beamforming relevant to phase alignment at the receiver; Phase alignment depends on carrier and packet syn-



Figure 1.1: Firefighter scenario

chronization and plays crucial role in the realization of power beamforming gains [3]. Concerning the distributed case, designer has to overcome certain adversities, since each terminal has its own oscillator and the network topology is usually unknown. Many algorithmic synchronization techniques have been proposed including multi-bit (or single-bit) closed-loop feedback between receiver and distributed transmitters, as described in [4–6]. Specifically, a master-slave architecture for achieving carrier synchronization was investigated in [7]; it was shown that with presence of phase errors on the order of  $60^\circ$ , signal-to-noise ratio (SNR) gains of 70% can be achieved. For further information about distributed beamforming the reader is directed to [8] and references therein. To the best of our knowledge, most prior art on distributed beamforming includes either CSI availability (e.g. [9]) or feedback (from the receiver) availability at the distributed transmitters or ability to access the transmitter radio module for carrier phase adjustments.

### 1.3 Thesis outline

The thesis studies distributed zero-feedback (i.e. blind) beamforming, assuming no CSI availability, no receiver-based feedback and simple, commodity WSN radios, where access to carrier phase adjustments is not possible. We are motivated by network partitioning problems, where a subset of nodes

---

is disconnected from the rest of the network, i.e. among the subset, each terminal cannot communicate with the nearest neighbor outside the subset, and thus, the subset is disconnected from the rest of the network (this is also known as the reachback communication problem). As a result, feedback from outside the subset cannot be received. Another problem includes emergency situations inside a building, when collaborative beamforming is needed to establish a reliable link and send information out of the building (i.e. Firefighter scenario—Fig. 1.1). Additionally, commodity radios are assumed, where no access to the transmitter carrier phase is feasible. Work in [10], [11] showed that zero-feedback beamforming with unsynchronized carrier is possible and provided information-theoretic analysis, in terms of signal alignment probability, signal alignment delay and respective beamforming gains. However, no specific receivers were proposed. Work on this thesis provides concrete non-coherent receivers for zero-feedback distributed beamforming, under the aforementioned assumptions.

Specifically, the thesis contributions of this are presented as follows:

- In Chapter 2, a heuristic, near-optimal receiver (in terms of bit error rate (BER)) based on repetition coding, is proposed and BER performance is evaluated via Monte-Carlo simulations.
- In Chapter 3, a non-coherent receiver based on maximum likelihood (ML) and interleaving is presented and its BER performance closed form is derived.
- In Chapter 4, unitary space-time constellations (USTCs) in the context of distributed terminals are examined and BER performance is offered.
- In Chapter 5 the conclusion is provided.



## Chapter 2

# Beamforming using repetition coding

This chapter introduces the idea of zero-feedback distributed beamforming and examines scenarios where the links between the receiver (destination) and all distributed transmitters (nodes) in a wireless network (i.e. wireless sensor network) are so weak; thus, pilot signals or feedback messages for channel estimation or any other type of receiver feedback messages cannot be assumed. Moreover, zero-feedback beamforming makes the problem more challenging without high cost software or special hardware equipment for synchronization. The first part presents the problem formulation, the signal model and the basic idea of the zero-feedback distributed beamforming gain based on an alignment event of the transmitted signals from distributed nodes. A note on probability of this alignment event is enclosed in this chapter and it is described in detail in [10]. The second part proposes a repetition coding scheme that exploits the alignment event, it includes a non-coherent detector and finally it offers the BER performance through simulations.

### 2.1 Signal model

$M$  distributed terminals transmit simultaneously a common information symbol towards a destination terminal that receives the superposition of their signals at a given frequency band (Fig. 2.1). Binary modulation is assumed, with signal set  $\mathcal{X} = \{x_0, x_1\}$ . From transmitter  $m \in \mathcal{T} \triangleq \{1, \dots, M\}$  to destination the model considers carrier frequency offset (CFO)  $\Delta f_m$ , Rayleigh, flat fading channel  $h_m = A_m e^{j\phi_m} \sim \mathcal{CN}(0, 1)$  and additive Complex White

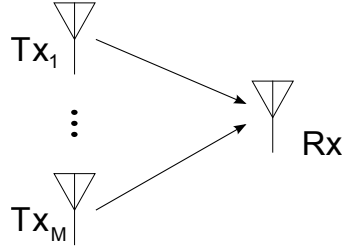


Figure 2.1: System model

Gaussian Noise (CWGN)  $w_k \sim \mathcal{CN}(0, \sigma^2)$ . The random variables  $\{h_m\}$  and  $\{\Delta f_m\}$  are independent for different  $m$ . Finally, the parameter  $T_s$  represents the symbol period and the model is expressed as follows:

$$y_k \triangleq \sum_{m=1}^M h_m e^{+j2\pi\Delta f_m k T_s} x_k + w_k = \tilde{x}_k + w_k, \quad (2.1)$$

where  $x_k \in \mathcal{X}$  denotes  $k^{\text{th}}$  information symbol.

Due to the fact that distributed transmitters are equipped with non-ideal local oscillators (i.e. manufacturing errors create offsets from the nominal oscillation frequency), a carrier frequency offset is added. We assume a zero-mean i.i.d normally distributed CFO parameter with standard deviation  $\sigma_f = \sqrt{\mathbb{E}\{\Delta f_m^2\}} = f_c \times \text{ppm}$ , where  $f_c$  is the nominal carrier frequency and ppm is the frequency skew of the clock crystals, with typical values of 1-20 parts per million (ppm). For example, clock crystals of 20 ppm provide a CFO on the order of  $2.4 \text{ GHz} \times 20 \cdot 10^{-6} = 48 \text{ kHz}$ . The channel is assumed to be constant for an exact number of symbol periods (time slots) determined by its coherence time  $\tau_c$ .  $L \triangleq \tau_c/T_s$  is defined as the maximum number of time slots, where the channel remains constant. We call “phase” the duration of  $L$  symbols after which, a new phase begins and the fading coefficients are completely changed and independent from the previous ones (quasi-static fading). CFO parameters are considered random but constant for the case of repetition coding (Ch. 2) and interleaving (Ch. 3) schemes. Throughout this thesis, on-off keying (OOK) modulation is assumed, where the binary signal set becomes  $\mathcal{X} = \{x_0, x_1\}$ , with  $x_0 = 0$  and  $x_1 = \sqrt{E_1}$

equiprobable symbols. The average SNR per  $m^{\text{th}}$  transmitter antenna per  $k^{\text{th}}$  time slot is defined as:

$$\text{SNR} \triangleq \frac{\mathbb{E}[x_k^2]}{\mathbb{E}[|w_k|^2]} = \frac{E_1}{2\sigma^2}. \quad (2.2)$$

## 2.2 Alignment probability of $M$ signals

### 2.2.1 Alignment event

The basic idea of zero-feedback distributed beamforming is based on signal alignment at the destination terminal exploiting constructive gain for power maximization. Specifically, the received signal power according to Eq. 2.1 is given by:

$$\begin{aligned} |\tilde{x}_k|^2 &= \left| x_k \cdot \left( \sum_{m=1}^M h_m e^{+j2\pi\Delta f_m k T_s} \right) \right|^2 \\ &= x_k^2 \cdot \left| \left( \sum_{m=1}^M A_m e^{+j(2\pi\Delta f_m k T_s + \phi_m)} \right) \right|^2 \\ &= x_k^2 \cdot \left\{ \sum_{m=1}^M A_m^2 + \right. \\ &\quad \left. + 2 \sum_{m \neq i} A_m A_i \cos(2\pi(\Delta f_m - \Delta f_i) k T_s + \phi_m - \phi_i) \right\} \\ &= x_k^2 \cdot \text{L}_{\text{BF}}[k]. \end{aligned} \quad (2.3)$$

It is noticeable that the cosine terms inside the braces are positive or negative, depending on  $\{\Delta f_m\}$ ,  $m \in \mathcal{T}$ , CFO parameter and phase offset  $\phi_m$ . The signs of the cosines lead to constructive or destructive beamforming factor  $\text{L}_{\text{BF}}[k]$ . We give an example of a perfect constructive addition of the signals. Let two distributed transmitters ( $M = 2$ ) have carrier frequency offsets  $\Delta f_2 = 2\Delta f_1 = f_0$  and their signals arrive at the destination with phase difference  $\pi/2$  at time instant  $t = t_0$  (see Fig. 2.2). It can be easily seen that at time  $t = t_0 + 0.5/f_0$  the signals (phasors) of the two distributed trans-

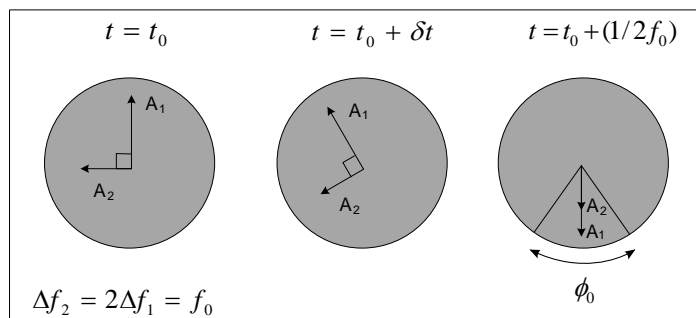


Figure 2.2: Alignment

mitters will be aligned in a sector  $\phi_0$ . This implies that a repetition scheme has a probability to create an alignment event. The work in [10] studies the alignment probability of  $M$  signals for any  $M$ -dimensional phase offset vector  $\bar{\phi} = [\phi_1, \dots, \phi_M]^T$  and any CFO distribution. Furthermore, the expected number of symbols where alignment occurs and the required average length of repetition are also discussed.

Specifically, an alignment event is defined as the constructive addition of the signals which are enclosed in a sector  $\phi_0 = \cos^{-1}(a)$ , where the alignment parameter  $a \in (0, 1]$ . This event is mathematically expressed as:

$$\text{Align}[k, a, M] \triangleq \bigcap_{m \neq i} \left\{ \cos \left( \tilde{\phi}_m[k] - \tilde{\phi}_i[k] \right) \geq a \right\}, \quad (2.4)$$

where  $\tilde{\phi}_m[k] \triangleq 2\pi\Delta f_m k T_s + \phi_m$  and  $m, i \in \{1, \dots, M\}$ . The beamforming factor in Eq. 2.3 using the expression above becomes:

$$L_{\text{BF}}[k] \geq \sum_{m=1}^M A_m^2 + 2a \sum_{m \neq i} A_m A_i \in \mathcal{O}(M[1 + a(M-1)]).$$

For a perfect alignment ( $a=1$ ), the maximum value of the beamforming factor becomes  $\mathcal{O}(M^2)$ . This implies that we can have a maximum beamforming gain in the order of  $M^2$  in this scheme, when the phasors are perfectly aligned.

### 2.2.2 Alignment probability

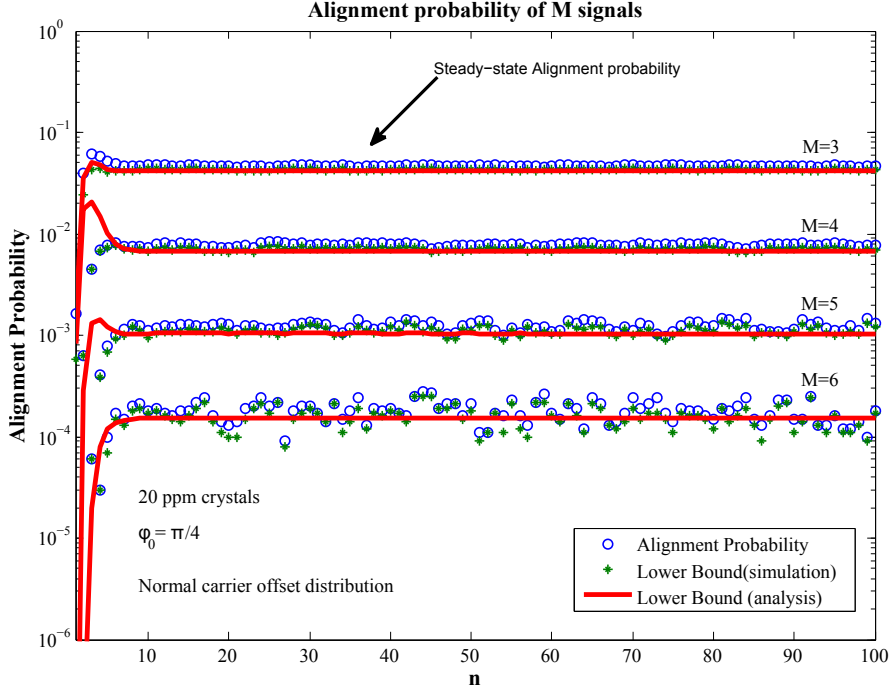
This subsection presents some results in [10, Section III]. Let a set  $S_M = \{1, \dots, M\}$ , then the lower bound of alignment probability is [10, Eq. 18]:

$$P \{ \text{Align} [k, a, M] \} \geq P \left\{ \max_{i \in S_M} \{ \check{\phi}_i [k] \} \leq \min_{i \in S_M} \{ \check{\phi}_i [k] \} + \phi_0 \right\}, \quad (2.5)$$

where  $\check{\phi}_i [k] \triangleq \tilde{\phi}_i [k] \bmod 2\pi = (2\pi\Delta f_i k T_s + \phi_i) \bmod 2\pi$  an independent non-identically distributed random variable in  $[0, 2\pi)$ ,  $\forall i \in \{1, \dots, M\}$ . The rv above is i.n.i.d, because of the different  $\{\phi_i\}'s$ . Additionally, the value of  $\phi_0$  is assumed to be restricted in  $[0, \pi/2)$ . This restriction considers cases for any  $k \in \mathbb{Z}$  and more specifically the intervals  $[2k\pi, 2k\pi + \pi/2)$  or  $(2k\pi - \pi/2, 2k\pi]$ . The RHS of Eq. 2.6 represents the lower bound, since there are cases of alignment event, when  $\max_{i \in S_M} \{ \check{\phi}_i [k] \} > 2\pi - \phi_0$  and  $\min_{i \in S_M} \{ \check{\phi}_i [k] \} < \phi_0$ , that are not captured by RHS. A lower bound closed form is presented in [10, Eq. 21] via numerical and analytical computations in [10, Appendix I] and is given by:

$$P \{ \text{Align} [k, a, M] \} \geq \int_{y=0}^{2\pi} \int_{x=y}^{\min\{y+\phi_0, 2\pi\}} p_{y,x}(y, x) dx dy, \quad (2.6)$$

where  $y = \min_{i \in S_M} \{ \check{\phi}_i [k] \}$ ,  $x = \max_{i \in S_M} \{ \check{\phi}_i [k] \}$  and  $p_{y,x}(y, x)$  denotes their joint pdf. For our case assuming zero-mean i.i.d normal distribution for  $\{\Delta f_m\}$ ,  $m \in \mathcal{T}$ , CFO parameter, the pdf is easily computed using [10, Eq. 19] and [10, Appendix I, Lemma 1]. The simulations results for alignment probability and its lower bound are depicted in 2.3. Beyond the simulations, an analysis based lower bound is added for showing that analysis and simulations are matched and the bound is tight. Finally, it is shown that alignment probability drops exponentially when the number  $M$  of transmitters is linearly increased [10, Eq. 22]. This result explains the fact that an alignment event of  $M$  phasors is more unlikely to happen, when the transmitters are increased.

Figure 2.3: Alignment probability vs time (symbol number  $n$ )

## 2.3 Protocol

Repetition coding exploits the fact that an alignment event can be occurred if an information symbol transmission is repeated, as referred above.  $M$  transmitters simultaneously transmit the same information symbol for  $L$  slots while the channel fading parameters remain constant. The achieved rate is  $1/L$  and the model becomes as follows (Fig. 2.4):

$$\mathbf{y} \triangleq \begin{bmatrix} y_1 \\ \vdots \\ y_l \\ \vdots \\ y_L \end{bmatrix} = \begin{bmatrix} \check{h}_1 \\ \vdots \\ \check{h}_l \\ \vdots \\ \check{h}_L \end{bmatrix} \cdot x + \begin{bmatrix} w_1 \\ \vdots \\ w_l \\ \vdots \\ w_L \end{bmatrix} = \check{\mathbf{h}}x + \mathbf{w}, \quad (2.7)$$

where  $\check{h}_l \triangleq \sum_{m=1}^M h_m e^{j2\pi\Delta f_m l T_s}$  given  $\{\Delta f_m\}$  is distributed according to the conditional pdf  $\sim f_{\check{\mathbf{h}}|\{\Delta f_m\}}(\check{\mathbf{h}} | \{\Delta f_m\}) \equiv \mathcal{CN}(0, M)$  as a linear combination

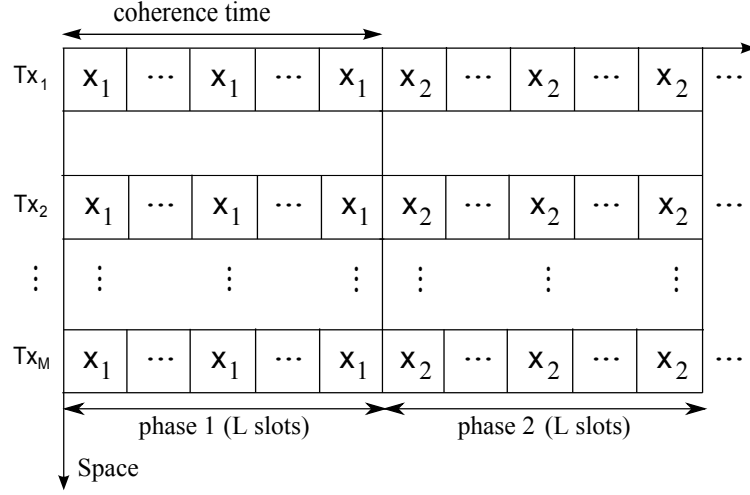


Figure 2.4: Repetition coding

of i.i.d  $h_m \sim \mathcal{CN}(0, 1)$ ,  $\forall l \in \{1, \dots, L\}$ . The noise vector elements are i.i.d  $w_l \sim \mathcal{CN}(0, \sigma^2)$  for  $l \in \{1, \dots, L\}$ .

## 2.4 Non-coherent detector

According to Eq. (2.7) and the system assumptions, the binary hypothesis test is given by:

$$\begin{aligned} H_0 : \mathbf{y} &= \mathbf{w}, \\ H_1 : \mathbf{y} &= \check{\mathbf{h}}x_1 + \mathbf{w}. \end{aligned}$$

An alignment event is expected to be occurred during  $L$  symbol periods according to Subsection 2.2.2, thus a large  $L$  parameter is considered to exploit alignment probability. The alignment event provides a constructive gain which distinguishes signal from noise in a  $l^{th}$  time slot. However, a subset of the slots where signal alignment occurs is not a priori known. This leads to the adaption of a square law technique, where all  $L$  symbols are taken into

account:

$$\mathbf{y}^\dagger \mathbf{y} = \sum_{l=1}^L |y_l|^2. \quad (2.8)$$

Under  $H_0$ , the squared  $\mathcal{L}_2$  norm of  $\mathbf{y} \mid H_0 = \mathbf{w}$  is distributed according to Gamma distribution, as a sum of i.i.d exponentials:

$$H_0 : \mathbf{y}^\dagger \mathbf{y} = \sum_{l=1}^L |w_l|^2 = w \sim \mathcal{G}(L, \sigma^2). \quad (2.9)$$

Under  $H_1$  and for given  $\{\Delta f_m\}$ , the squared  $\mathcal{L}_2$  norm of  $\mathbf{y} \mid H_1$  is a sum of correlated, identically Gamma-distributed rvs:

$$H_1 \mid \{\Delta f_m\} : \mathbf{y}^\dagger \mathbf{y} = \sum_{l=1}^L |y_l|^2 = \sum_{l=1}^L \zeta_l, \quad \zeta_l \sim \mathcal{G}(L, Mx_1^2 + \sigma^2), \quad (2.10)$$

where the correlation coefficient  $\rho_{ij}$  ( $|\rho_{ij}| \leq 1$ ) between  $\zeta_i$  and  $\zeta_j$  for  $i \neq j$ ,  $i, j \in \{1, \dots, L\}$  is given by:

$$\begin{aligned} \rho_{ij} &= \frac{\text{cov}(\zeta_i, \zeta_j)}{\sqrt{\text{var}(\zeta_i) \text{var}(\zeta_j)}} \\ &= \frac{x_1^4 \left\{ M + 2 \sum_{k \neq n} \cos[2\pi T_s (\Delta f_k - \Delta f_n)(i - j)] \right\}}{(Mx_1^2 + \sigma^2)^2}. \end{aligned} \quad (2.11)$$

Assuming knowledge of the conditional pdf (i.e. given  $\{\Delta f_m\}$ ), the unconditional pdf of  $\mathbf{y}^\dagger \mathbf{y}$  under  $H_1$  can be calculated. A closed form for the pdf of the sum of correlated Gamma exists in [12, Eq. 5] and [13], offered as a function of the correlation matrix  $\mathbf{C}$ ,

$$\mathbf{C} = \begin{bmatrix} 1 & \sqrt{\rho_{12}} & \dots & \sqrt{\rho_{1L}} \\ \sqrt{\rho_{21}} & 1 & \dots & \sqrt{\rho_{2L}} \\ \vdots & & \dots & \dots \\ \sqrt{\rho_{L1}} & \sqrt{\rho_{L2}} & \dots & 1 \end{bmatrix} \quad (2.12)$$

for the special case where  $\mathbf{C}$  is positive definite. In our problem,  $\mathbf{C}$  is not necessarily positive definite and thus, relevant analytical results in [12], [13] are not applicable in this work. For example, consider the case of  $M = 2$ ,  $[\Delta f_1 \ \Delta f_2] = [-0.6479e5 \ 1.4568e5]$ , where

$$\mathbf{C} = \begin{bmatrix} 1.0000 & 0.6863 & 0.2138 & 0.3489 & 0.7645 & 0.8578 \\ 0.6863 & 1.0000 & 0.6863 & 0.2138 & 0.3489 & 0.7645 \\ 0.2138 & 0.6863 & 1.0000 & 0.6863 & 0.2138 & 0.3489 \\ 0.3489 & 0.2138 & 0.6863 & 1.0000 & 0.6863 & 0.2138 \\ 0.7645 & 0.3489 & 0.2138 & 0.6863 & 1.0000 & 0.6863 \\ 0.8578 & 0.7645 & 0.3489 & 0.2138 & 0.6863 & 1.0000 \end{bmatrix}.$$

Its eigenvalues are

$$[-0.0449 \ 0.0481 \ 0.1444 \ 1.0075 \ 1.2311 \ 3.6138]$$

and thus,  $\mathbf{C}$  is not positive definite.

Consider the above result, there is not an available pdf closed form for the case of  $\mathbf{y}^\dagger \mathbf{y}$  under  $H_1$ . However, a suboptimal method can be used for the detection threshold of the binary test, based on known statistics under  $H_0$ , since a ML detector cannot be derived. The non-coherent detector is given by:

$$\mathbf{y}^\dagger \mathbf{y} = \sum_{l=1}^L |y_l|^2 \stackrel{H_1}{\geq} \theta(k). \quad (2.13)$$

An appropriate value for threshold  $\theta$  is based on minimization of the probability of error under  $H_0$  ( $P(e | H_0)$ ), i.e. the error of deciding  $x_1$  was transmitted instead of  $x_0$ . This error occurs when there are large noise values for some received samples that their sum can be detected as constructive addition of transmitted signals. Thus, threshold must be selected sufficiently large such that the probability of error under  $H_0$  is minimized. The threshold represents an approximation of the maximum value of squared  $\mathcal{L}_2$  norm of  $\mathbf{y}$  under  $H_0$ , considering the first and second order statistics of  $w$  and is given

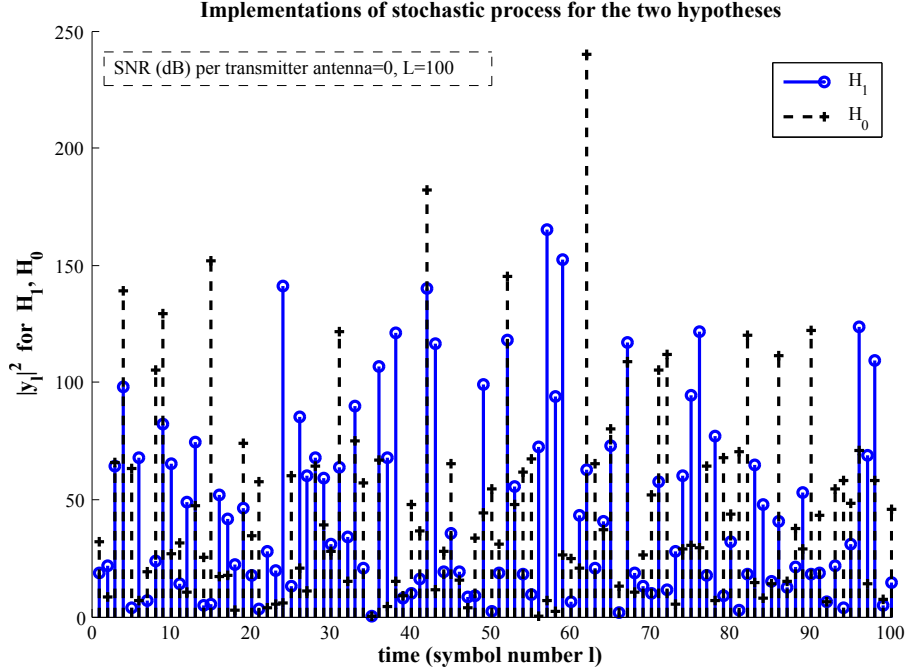


Figure 2.5: Independent random implementation of  $|y_l|^2$  for the two hypotheses (SNR (dB) per transmitter antenna = 0)

by:

$$\theta(k) \simeq \mathbb{E}[w] + k\sqrt{\text{var}[w]} = \sigma^2 \left[ L + k\sqrt{L} \right], \quad k > 0, \quad (2.14)$$

where  $k$  parameter considers the Gamma distribution positive skewness, since the increment of  $k$  approximates better the maximum value of  $w$  follows the Gamma distribution tail. The  $k$  parameter is selected through simulation, in order to minimize the probability of error. To find an upper bound of parameter  $k$  only considering the hypothesis  $H_0$ , the  $P(e | H_0)$  must be:

$$\begin{aligned} P(e | H_0) \leq \epsilon &\Leftrightarrow \int_{\theta(k)}^{+\infty} \frac{1}{(\sigma^2)^L} \frac{1}{(L-1)!} x^{L-1} e^{-\frac{x}{\sigma^2}} dx \leq \epsilon \\ &\Leftrightarrow \frac{1}{(L-1)!} \Gamma\left(L, \frac{\theta(k)}{\sigma^2}\right) \leq \epsilon, \end{aligned} \quad (2.15)$$

where i.e.  $\epsilon = 10^{-6}$  and  $\Gamma(a, z) = \Gamma(a) - \gamma(a, z) = \int_z^{+\infty} t^{a-1} e^{-t} dt$ ;  $\Re(a) > 0$ ,  $\gamma(a, z)$  is the incomplete Gamma function [14, p. 260, Eq. 6.5.2] and  $\Gamma(a)$  is

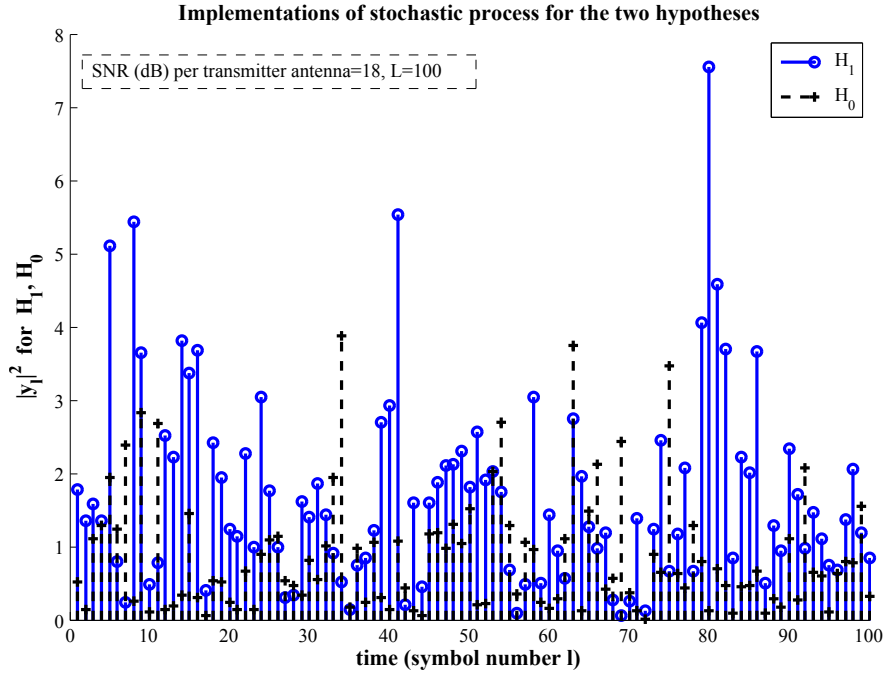


Figure 2.6: Independent random implementation of  $|y_l|^2$  for the two hypotheses (SNR (dB) per transmitter antenna = 18)

the Gamma function [14, p. 255, Eq. 6.1.1]. The  $k$  parameter selection does not optimize the overall bit-error-rate (BER), since  $P(e | H_1)$  is not taken into account. Thus, near-optimal parameter  $k$  is evaluated, considering both  $P(e | H_1)$  and  $P(e | H_0)$ .

## 2.5 Simulation

The numerical results assume  $f_c = 2.4$  GHz,  $T_s = 1 \mu s$  and 20 ppm clock crystals. For single symbol and repetition coding distributed beamforming transmission, the same total transmission power per antenna terminal is assumed, thus:

$$\frac{E_1^s}{2\sigma^2} = \frac{LE_1^r}{2\sigma^2} \triangleq \text{SNR per transmitter antenna},$$

where  $E_1^s, E_1^r$  denote the transmission power of symbol  $x_1$  for single symbol and interleaving distributed beamforming transmission respectively. The

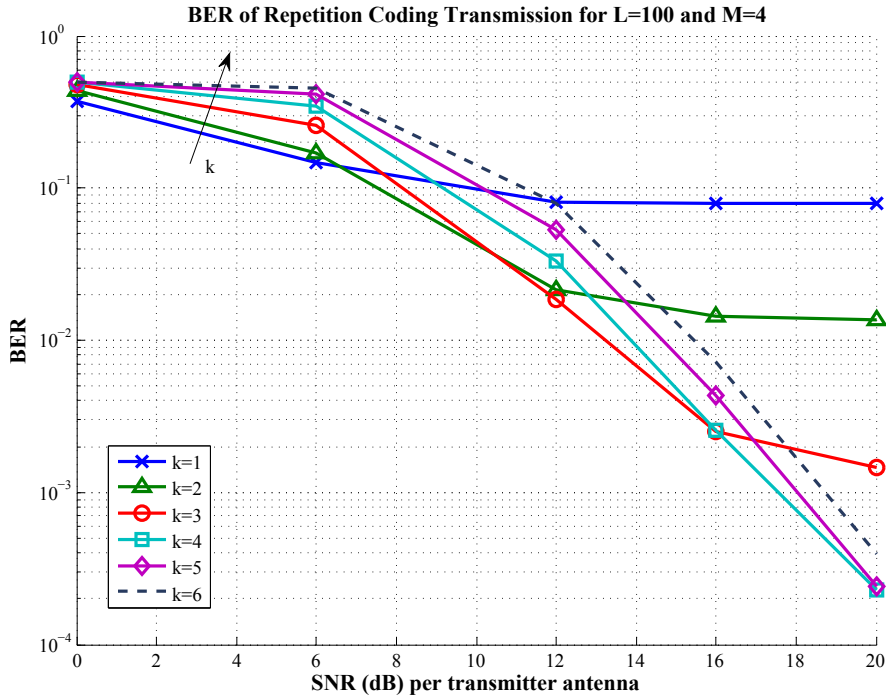


Figure 2.7: Proper  $k$  parameter selection for repetition coding

equation above provides meaningful performance comparison for the different systems.

Fig. 2.7 depicts BER vs SNR per transmitter antenna, for  $M = 4$  distributed terminals and  $L = 100$  symbols, as a function of different values of threshold  $\theta(k)$ . The evaluation of threshold  $\theta(k)$  depends on positive integer values of  $k$  according to Eq. 2.14, because of the small variation of BER for  $\theta(k)$  and  $\theta(k+1)$ , also evident from 2.7. Considering Eq. 2.15, an upper bound of  $k$  is found for a given  $\epsilon$  (i.e.  $k_{\text{upper}} = 6$  for  $\epsilon = 10^{-6}$ ). Thus, the simulation considers  $k \leq k_{\text{upper}}$  and is noticeable that is not optimal for overall BER, since this bound considers probability error minimization only under  $H_0$ . On the other hand, a large value of  $k$  results to a larger value of  $\theta(k)$  and smaller probability of deciding  $H_0$  in favor of hypothesis  $H_1$ . Different values of positive integer  $k$  are appropriate for different SNR regimes; for SNR per transmitter antenna of 2 – 6 dB, 10 – 16 dB and 16 – 20 dB, the appropriate value of positive integer  $k$  that minimizes BER is  $k = 1$ ,  $k = 3$  and  $k = 4$ , respectively, for the specific values of  $L$  and  $M$ . The sufficient statistic  $\mathbf{y}^\dagger \mathbf{y}$

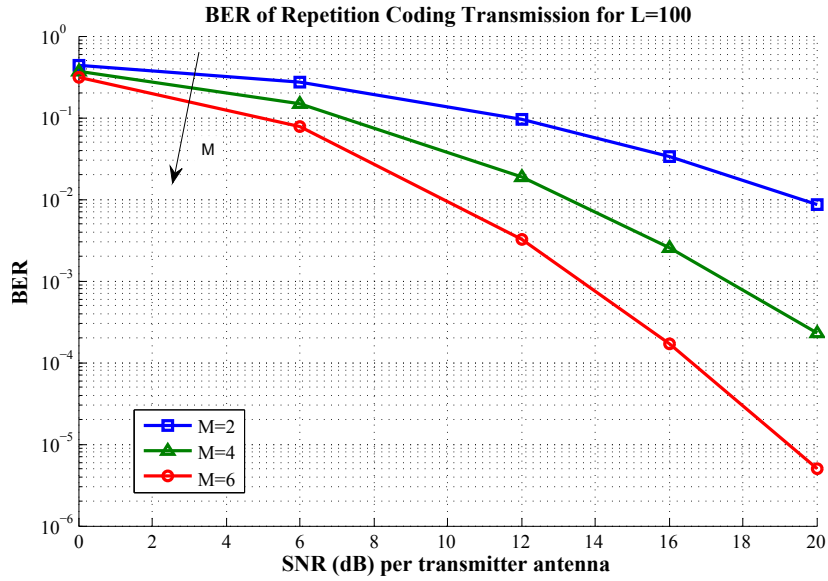


Figure 2.8: Simulation BER performance using proper  $k$  parameter with different number of transmitters

of Eq. 2.13 can be large because of a large value of a single (or more) noise sample(s) or a signal alignment; thus, low SNR requires a smaller threshold  $\theta(k)$  as opposed to higher SNR regimes, as also evident from (Fig. 2.5, Fig. 2.6), such that  $\mathbf{y}^\dagger \mathbf{y}$  for the case of aligned signal under  $H_1$  does not fall below the threshold, i.e. probability of error under  $H_1$  is kept small, through an appropriate threshold  $\theta(k)$  that adapts to increases of the SNR value. This technique offers a systematic way to evaluate near-optimal  $k$  parameter for minimizing overall BER for specific SNR,  $L$  and  $M$  values. In Fig. 2.8, BER is plotted as a function of SNR per transmitter antenna and number  $M$  of distributed transmitters for fixed  $L = 100$  symbols. For different SNR and  $M$  values the above technique for  $k$  parameter selection was used. Despite the fact that signal alignment occurs with smaller probability, which decreases exponential with  $M$  [10]; BER is decreased with the increment of number  $M$  of transmitters at the expense of total transmission power, since repetition with  $M = 6$  transmitters consumes additional power, compared to the other two depicted cases of  $M = 2$  and  $M = 4$  (e.g. 50% more transmission power of  $M = 6$  compared to  $M = 4$ ). Therefore, there are cases (i.e. reachback communication problem in WSNs), where a trade-off between

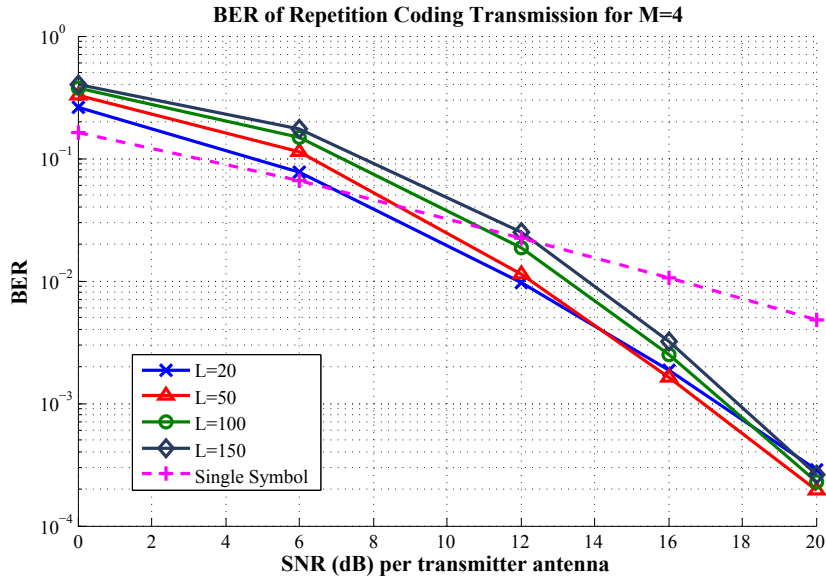


Figure 2.9: Simulation BER performance in different  $L$  time intervals

total transmission power and reachability of the adjacent nodes is existed. Instead, unconnected distributed terminals could collaborate for constructive addition at zero-feedback beamforming scenarios. Finally, in Fig. 2.9,<sup>2</sup> the number of transmitters is fixed to  $M = 4$  and the number of slots  $L$  is varied. It can be seen that for high SNR per transmitter antenna, a large value of  $L$  reduces BER, while for small SNR, a larger value of  $L$  increases BER. This can be intuitively explained, since a large  $L$  value may increase the expected number of slots (symbols) where signal alignment occurs. On the other hand, a large  $L$  value selection increases the probability that one received symbol is "hit" by significant noise power, offering respectively a large value for the observation  $\mathbf{y}^\dagger \mathbf{y}$ . This phenomenon will be observed because of noise and not because of signal alignment, especially at the low SNR regime.

<sup>2</sup>The single symbol depicted case refers to the analysis in Section 3.4.

## Chapter 3

# Beamforming using interleaving

In this chapter we propose an alternative protocol to the repetition coding protocol of Chapter 2 aiming to exploit diversity. An easy-to-implement non-coherent receiver based on maximum likelihood (ML) and interleaving is proposed and its BER performance is evaluated in closed form.

### 3.1 Protocol

This protocol consists of  $N$  phases; during each phase, the same  $L$  symbols are transmitted, with the same order (Fig. 3.1). Due to the quasi-static assumption, the wireless channel has changed at every phase, promising diversity benefits, at the expense of additional delay, since  $N$  blocks of the same  $L$  symbols need to be transmitted. The  $L$  symbols  $x_l$ ,  $l \in \{1, \dots, L\}$  are in principle different and thus, the overall rate is  $L/NL = 1/N$  (as opposed to the  $1/L$  of the simple repetition protocol discussed in Ch. 2). Thus, each information symbol  $x_l$ , ( $l \in \{1, \dots, L\}$ ) is transmitted  $N$  times, once at every phase. The received samples that correspond to information symbol  $x_l$  are given by the  $N \times 1$  vector:

$$\mathbf{y}_l = \begin{bmatrix} y_l \\ \vdots \\ y_{(n-1) \times L + l} \\ \vdots \\ y_{(N-1) \times L + l} \end{bmatrix},$$

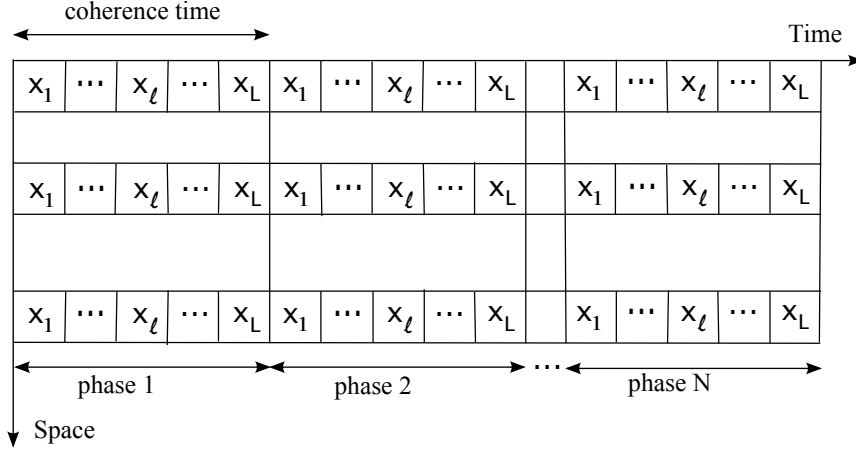


Figure 3.1: Interleaving

where the  $n^{\text{th}}$  element ( $n \in \{1, \dots, N\}$ ) of vector  $\mathbf{y}_l$  is given by:

$$Y_{(n-1) \times L+l} \triangleq \bar{h} \cdot X_{(n-1) \times L+l} + W_{(n-1) \times L+l},$$

with

$$\bar{h} \triangleq \sum_{m=1}^M h_m^{(n-1) \times L+l} \cdot e^{+j2\pi\Delta f_m[(n-1) \times L+l]T_s}.$$

For notational simplicity the  $l$  index can be dropped, since processing for each  $l$  is the same. Specifically,  $\forall l \in \{1, \dots, L\}$ , the definitions below are considered:

1. The  $n^{\text{th}}$  received sample,  $n \in \{1, \dots, N\}$  is denoted by:

$$y_n \triangleq Y_{(n-1) \times L+l}.$$

2. The channel coefficient for the  $m^{\text{th}}$  transmitter and the  $n^{\text{th}}$  sample:

$$h_m^n \triangleq h_m^{(n-1) \times L+l},$$

where  $h_m^n \sim \mathcal{CN}(0, 1)$  and  $\{h_m^n\}$  i.i.d across different  $m, n$ .

3. The  $n^{\text{th}}$  receiver complex white Gaussian noise sample:

$$w_n \triangleq \mathbf{w}_{(n-1) \times L + l},$$

where  $w_n \sim \mathcal{CN}(0, \sigma^2)$  and  $\{w_n\}$  i.i.d.

4. The same information symbol  $x$  for all  $N$  phases:

$$x \triangleq \mathbf{x}_{(n-1) \times L + l}, \quad \forall n \in \{1, \dots, N\}.$$

Consequently, the  $n^{\text{th}}$  element becomes:

$$\begin{aligned} y_n &= x \cdot \left( \sum_{m=1}^M h_m^n e^{+j2\pi\Delta f_m[(n-1) \times L + l]T_s} \right) + w_n, \\ y_n &= \tilde{h}_n x + w_n, \end{aligned}$$

where  $\tilde{h}_n \triangleq \sum_{m=1}^M h_m^n e^{+j2\pi\Delta f_m[(n-1) \times L + l]T_s}$ .

For completeness to the following theorem proof, the reader is directed to a useful definition and a theorem for proper complex Gaussian random vectors in Appendix A.

The following theorem shows that the statistics of the random variable  $\tilde{h}_n$  do not depend on the CFOs  $\Delta f_m$ .

**Theorem 1.** *The random variables  $\tilde{h}_n$  and  $\tilde{h}_k$  ( $n \neq k$  and  $n, k \in \{1, \dots, N\}$ ) are i.i.d and distributed according to  $\mathcal{CN}(0, M)$ .*

*Proof.* For  $n \neq k$ , the following vectors are defined:

$$\mathbf{h} \triangleq \begin{bmatrix} h_1^n \\ \vdots \\ h_M^n \\ h_1^k \\ \vdots \\ h_M^k \end{bmatrix} = \begin{bmatrix} \mathbf{h}^n \\ \mathbf{h}^k \end{bmatrix},$$

where  $\mathbf{h} \sim \mathcal{CN}(\mathbf{0}_{2M}, \mathbf{I}_{2M})$  and  $\mathbf{h}^i = [h_1^i \cdots h_M^i]^T \sim \mathcal{CN}(\mathbf{0}_M, \mathbf{I}_M)$  is proper subvector ( $i \in \{n, k\}$ ). We define the following random vector :

$$\hat{\mathbf{h}} \triangleq [\tilde{h}_n \ \tilde{h}_k]^T = \mathbf{E} \cdot [\mathbf{h}^n \ \mathbf{h}^k]^T = \mathbf{E} \cdot \mathbf{h}, \quad (3.1)$$

where

$$\mathbf{E} \triangleq \begin{bmatrix} \mathbf{e}_n & \mathbf{0}_M \\ \mathbf{0}_M & \mathbf{e}_k \end{bmatrix}^T,$$

is a  $2 \times 2M$  matrix and

$$\mathbf{e}_i \triangleq [e^{+j2\pi\Delta f_1[(i-1) \times L+l]T_s} \cdots e^{+j2\pi\Delta f_M[(i-1) \times L+l]T_s}]^T,$$

is a  $M \times 1$  vector, with  $i \in \{n, k\}$ .

**Lemma 1.** *Let  $\mathbf{v}$  be a proper complex  $n$ -dimensional random vector[15], i.e.,  $\mathbf{M}_{\mathbf{v}} = \mathbb{E} [(\mathbf{v} - \mathbb{E}[\mathbf{v}]) (\mathbf{v} - \mathbb{E}[\mathbf{v}])^T] = \mathbf{O}_n$ . Then any random vector obtained from  $\mathbf{v}$  by a linear affine transformation, i.e., any random vector  $\mathbf{q}$  of the form  $\mathbf{q} = \mathbf{A}\mathbf{v} + \mathbf{b}$ , where  $\mathbf{A} \in \mathbb{C}^{m \times n}$  and  $\mathbf{b} \in \mathbb{C}^m$  are constant, is also proper.*

Using Lemma 1 and Eq. 3.1,  $\hat{\mathbf{h}}$  conditioned on  $\mathbf{E}$  is a proper complex

Gaussian vector with mean vector and covariance matrix, as follows:

$$\begin{aligned}\mathbb{E}_{\hat{\mathbf{h}}|\mathbf{E}}\left[\hat{\mathbf{h}} \mid \mathbf{E}\right] &= \mathbf{0}_2, \\ \mathbb{E}_{\hat{\mathbf{h}}|\mathbf{E}}\left[\left(\hat{\mathbf{h}} - \mathbb{E}_{\hat{\mathbf{h}}|\mathbf{E}}\left[\hat{\mathbf{h}}\right]\right)\left(\hat{\mathbf{h}} - \mathbb{E}_{\hat{\mathbf{h}}|\mathbf{E}}\left[\hat{\mathbf{h}}\right]\right)^\dagger \mid \mathbf{E}\right] &= M\mathbf{I}_2.\end{aligned}$$

Consequently,  $f_{\hat{\mathbf{h}}|\mathbf{E}}(\hat{\mathbf{h}} \mid \mathbf{E}) \sim \mathcal{CN}(\mathbf{0}_2, M\mathbf{I}_2)$  conditioned on  $\mathbf{E}$ .

We denote as  $\mathbf{e} \triangleq \mathbf{vec}(\mathbf{E})$  and as  $f_{\mathbf{e}}(\mathbf{e})$  the joint distribution of all the entries of matrix  $\mathbf{E}$ , hence:

$$f_{\hat{\mathbf{h}}}(\hat{\mathbf{h}}) = \mathbb{E}_{\mathbf{e}}\left[f_{\hat{\mathbf{h}}|\mathbf{e}}(\hat{\mathbf{h}} \mid \mathbf{e})\right] = \int_{-\infty}^{+\infty} f_{\hat{\mathbf{h}}|\mathbf{e}}(\hat{\mathbf{h}} \mid \mathbf{e})f_{\mathbf{e}}(\mathbf{e})d\mathbf{e}. \quad (3.2)$$

Using Theorem 2  $f_{\hat{\mathbf{h}}|\mathbf{e}}(\hat{\mathbf{h}} \mid \mathbf{e})$  is given by:

$$f_{\hat{\mathbf{h}}|\mathbf{e}}(\hat{\mathbf{h}} \mid \mathbf{e}) = \frac{1}{(\pi M)^2} \exp\left(-\frac{\|\hat{\mathbf{h}}\|_2^2}{M}\right).$$

The expression above can be taken out of the integral of Eq.(3.2), since is independent of  $\mathbf{e}$ :

$$f_{\hat{\mathbf{h}}}(\hat{\mathbf{h}}) = f_{\hat{\mathbf{h}}|\mathbf{e}}(\hat{\mathbf{h}} \mid \mathbf{e}) \int_{-\infty}^{+\infty} f_{\mathbf{e}}(\mathbf{e})d\mathbf{e} = f_{\hat{\mathbf{h}}|\mathbf{e}}(\hat{\mathbf{h}} \mid \mathbf{e}).$$

As a result,  $\hat{\mathbf{h}} \sim \mathcal{CN}(\mathbf{0}_2, M\mathbf{I}_2)$  and  $\tilde{h}_n, \tilde{h}_k$  are i.i.d and distributed according to  $\sim \mathcal{CN}(0, M)$ .  $\square$

Exploiting Theorem 1, the signal is simplified to:

$$\mathbf{y} = \tilde{\mathbf{h}}x + \mathbf{w}, \quad (3.3)$$

where  $\tilde{\mathbf{h}} \triangleq [\tilde{h}_1 \dots \tilde{h}_N]^T \sim \mathcal{CN}(\mathbf{0}_N, M\mathbf{I}_N)$  and  $\mathbf{w} \sim \mathcal{CN}(\mathbf{0}_N, \sigma^2\mathbf{I}_N)$ . The  $\tilde{\mathbf{h}}$  is a proper complex Gaussian random vector, since its elements are i.i.d complex vector random variables. Its joint distribution belongs to the same family of

distribution described by Theorem 2 and is given by:

$$f_{\tilde{\mathbf{h}}}(\tilde{\mathbf{h}}) \stackrel{\text{i.i.d.}}{=} \prod_{n=1}^N f_{\tilde{h}_n}(\tilde{h}_n) = \frac{1}{(\pi M)^N} \exp\left(-\frac{\|\tilde{\mathbf{h}}\|_2^2}{M}\right).$$

## 3.2 Coherent Detection

### 3.2.1 ML coherent detector

Assuming OOK modulation and according to Eq. 3.3 the hypothesis test is given by:

$$\begin{aligned} H_0 : \mathbf{y} &= \mathbf{w}, \\ H_1 : \mathbf{y} &= \tilde{\mathbf{h}}x_1 + \mathbf{w}. \end{aligned}$$

Conditioned on  $\tilde{\mathbf{h}}, H_i$ , with  $i \in \{0, 1\}$ ,  $\mathbf{y}$  is a proper complex Gaussian random vector as a linear affine transformation of the proper complex random vector  $\mathbf{w}$  with mean vector and covariance matrix, as follows:

$$\begin{aligned} \mathbb{E}_{\mathbf{w}}[\mathbf{y} | \tilde{\mathbf{h}}, H_i] &= \mathbb{E}_{\mathbf{w}}[\tilde{\mathbf{h}}x_i + \mathbf{w} | \tilde{\mathbf{h}}, H_i] = \tilde{\mathbf{h}}x_i, \\ \mathbb{E}_{\mathbf{w}}[(\mathbf{y} - \mathbb{E}_{\mathbf{w}}[\mathbf{y}]) (\mathbf{y} - \mathbb{E}_{\mathbf{w}}[\mathbf{y}])^\dagger | \tilde{\mathbf{h}}, H_i] &= \mathbb{E}_{\mathbf{w}}[\mathbf{w}\mathbf{w}^\dagger | \tilde{\mathbf{h}}, H_0] = \sigma^2 \mathbf{I}_N, \end{aligned}$$

for  $i \in \{0, 1\}$ .

Thus,

$$f_{\mathbf{y} | \tilde{\mathbf{h}}, H_0}(\mathbf{y} | \tilde{\mathbf{h}}, H_0) = \frac{1}{(\pi\sigma^2)^N} \exp\left(-\frac{\|\mathbf{y}\|_2^2}{\sigma^2}\right), \quad (3.4)$$

$$f_{\mathbf{y} | \tilde{\mathbf{h}}, H_1}(\mathbf{y} | \tilde{\mathbf{h}}, H_1) = \frac{1}{(\pi\sigma^2)^N} \exp\left(-\frac{\|\mathbf{y} - \tilde{\mathbf{h}}x_1\|_2^2}{\sigma^2}\right). \quad (3.5)$$

Applying MAP and assuming equiprobable symbols and  $x, \tilde{\mathbf{h}}$  independent, the receiver design concludes to a ML coherent detector given by:

$$\begin{aligned} \hat{H}_i \text{ such that } i &= \arg \max_{j \in \{0,1\}} P(H_j | \mathbf{y}, \tilde{\mathbf{h}}) \\ &= \arg \max_{j \in \{0,1\}} \frac{f_{\mathbf{y}|\tilde{\mathbf{h}},H_j}(\mathbf{y} | \tilde{\mathbf{h}}, H_j) f_{\tilde{\mathbf{h}}}(\tilde{\mathbf{h}}) P(H_j)}{f_{\mathbf{y},\tilde{\mathbf{h}}}(\mathbf{y}, \tilde{\mathbf{h}})} \\ &= \arg \max_{j \in \{0,1\}} f_{\mathbf{y}|\tilde{\mathbf{h}},H_j}(\mathbf{y} | \tilde{\mathbf{h}}, H_j). \end{aligned}$$

Consequently, after simple calculations, the ML detector is simplified to:

$$\begin{aligned} f_{\mathbf{y}|\tilde{\mathbf{h}},H_1}(\mathbf{y}|\tilde{\mathbf{h}}, H_1) &\stackrel{H_1}{\geq} f_{\mathbf{y}|\tilde{\mathbf{h}},H_0}(\mathbf{y}|\tilde{\mathbf{h}}, H_0) \Leftrightarrow \\ \frac{1}{(\pi\sigma^2)^N} e^{-\frac{\|\mathbf{y}-\tilde{\mathbf{h}}x_1\|_2^2}{\sigma^2}} &\stackrel{H_1}{\geq} \frac{1}{(\pi\sigma^2)^N} e^{-\frac{\|\mathbf{y}-\tilde{\mathbf{h}}x_0\|_2^2}{\sigma^2}} \Leftrightarrow \\ \|\mathbf{y}-\tilde{\mathbf{h}}x_1\|_2^2 &\stackrel{H_1}{\leq} \|\mathbf{y}-\tilde{\mathbf{h}}x_0\|_2^2 \Leftrightarrow \\ (\mathbf{y}-\tilde{\mathbf{h}}x_1)^\dagger (\mathbf{y}-\tilde{\mathbf{h}}x_1) &\stackrel{H_1}{\leq} \mathbf{y}^\dagger \mathbf{y} \Leftrightarrow \\ 2\Re(\tilde{\mathbf{h}}^\dagger \mathbf{y} x_1) &\stackrel{H_1}{\geq} \|\tilde{\mathbf{h}}\|_2^2 x_1^2 \Leftrightarrow \\ \Re\left(\frac{\tilde{\mathbf{h}}^\dagger \mathbf{y}}{\|\tilde{\mathbf{h}}\|_2^2}\right) &\stackrel{H_1}{\geq} \frac{x_1}{2}. \end{aligned}$$

### 3.2.2 BER performance analysis

For average BER evaluation, the following Lemma is needed:

**Lemma 2.** *For the case of vector detection in CWGN[16, p.508, Eq. A.53], the signal model is assumed to be:*

$$\mathbf{y} = \mathbf{u} + \mathbf{w},$$

where  $\mathbf{u} \in \mathbb{C}^K$  and  $\mathbf{w} \sim \mathcal{CN}(\mathbf{0}_K, N_0 \mathbf{I}_K)$ .

If vector  $\mathbf{u}$  is either  $\mathbf{u}_0 \in \mathbb{C}^K$  or  $\mathbf{u}_1 \in \mathbb{C}^K$ , then the error probability  $P(e)$  is

given by:

$$P(e) = Q\left(\frac{\|\mathbf{u}_0 - \mathbf{u}_1\|_2}{2\sqrt{N_0/2}}\right).$$

□

Applying Lemma 2 for our signal model, the  $P(e|\tilde{h})$  is given by:

$$P(e|\tilde{h}) = Q\left(\frac{\|\tilde{\mathbf{h}}\|_2 |x_0 - x_1|}{\sqrt{2\sigma^2}}\right) = Q\left(\sqrt{\text{SNR}} \|\tilde{\mathbf{h}}\|_2\right).$$

Taking expectation over  $\tilde{h}$ , the average BER is:

$$P(e) = \mathbb{E}_{\tilde{\mathbf{h}}} \left[ Q\left(\sqrt{\text{SNR}} \|\tilde{\mathbf{h}}\|_2\right) \right] = \mathbb{E}_{\tilde{\mathbf{h}}} \left[ Q\left(\sqrt{\text{SNR} \sum_{n=1}^N |\tilde{h}_n|^2}\right) \right].$$

The squared  $\mathcal{L}_2$  norm  $\|\tilde{\mathbf{h}}\|_2^2$  is a sum of i.i.d  $2N$  squared rvs  $\sim \mathcal{N}(0, \frac{M}{2})$ , thus is distributed according to  $\sim \mathcal{G}(N, M)$ .

Based on the above, the average BER becomes:

$$P(e) = \mathbb{E}_{\tilde{\mathbf{h}}} \left[ Q\left(\sqrt{\text{SNR} \sum_{n=1}^N |\tilde{h}_n|^2}\right) \right] = \mathbb{E}_x \left[ Q\left(\sqrt{\text{SNR} x}\right) \right] \Leftrightarrow$$

$$\begin{aligned} P(e) &= \int_0^{+\infty} Q\left(\sqrt{\text{SNR} x}\right) \frac{1}{M^N} \cdot \frac{1}{(N-1)!} \cdot x^{N-1} \cdot e^{-\frac{x}{M}} dx \\ &= \frac{1}{(N-1)!} \int_0^{+\infty} Q\left(\sqrt{(M \cdot \text{SNR}) y}\right) y^{N-1} e^{-y} dy. \end{aligned}$$

This has a well-known closed form, which is given by [16, p.62, Eq. 3.37]:

$$\frac{1}{(N-1)!} \int_0^{+\infty} Q(\sqrt{ay}) y^{N-1} e^{-y} dy = \left(\frac{1-\mu}{2}\right)^N \sum_{n=0}^{N-1} \binom{N-1+n}{n} \left(\frac{1+\mu}{2}\right)^n,$$

where  $\mu = \sqrt{\frac{a}{2+a}}$  .

Consequently, the average BER is simplified to:

$$P(e) = \left(\frac{1-\mu}{2}\right)^N \sum_{n=0}^{N-1} \binom{N-1+n}{n} \left(\frac{1+\mu}{2}\right)^n, \quad (3.6)$$

where  $\mu = \sqrt{\frac{M \cdot \text{SNR}}{2+M \cdot \text{SNR}}}$  .

### 3.2.3 Diversity

In this subsection, an asymptotic analysis of Eq. 3.6 is presented for studying the diversity order of the system discussed in the previous subsection.

For high transmit SNR we define  $\Delta x = \frac{2}{M \cdot \text{SNR}}$ ,  $f(x) = \sqrt{\frac{1}{x}}$  and  $f'(x) = -\frac{1}{2}x^{-\frac{3}{2}}$ .

Using first order Taylor approximation for  $x$  near 1, it can be proven that:

$$f(1 + \Delta x) = f(1) + f'(1)\Delta x + \mathcal{O}(|\Delta x|^2) = 1 - \frac{1}{M \cdot \text{SNR}} + \mathcal{O}(|\Delta x|^2)$$

Thus, the term  $\mu$  in Eq. 3.6 can be approximated as [16, p.55, Eq. 3.20]:

$$\mu = \sqrt{\frac{M \cdot \text{SNR}}{2 + M \cdot \text{SNR}}} \simeq 1 - \frac{1}{M \cdot \text{SNR}}.$$

As a result, the expressions below can be approximated for  $\text{SNR} \rightarrow +\infty$  as [16, pp.62-63]:

$$\frac{1+\mu}{2} \simeq 1, \quad (3.7)$$

$$\frac{1-\mu}{2} = \frac{1}{2} \left(1 - \sqrt{\frac{M \cdot \text{SNR}}{2 + M \cdot \text{SNR}}}\right) \simeq \frac{1}{2} \left(\frac{1}{M \cdot \text{SNR}}\right). \quad (3.8)$$

It can be easily seen that:

$$\begin{aligned} \sum_{n=0}^{N-1} \binom{N-1+n}{n} &= \sum_{n=N-1}^{2(N-1)} \binom{n}{n-(N-1)} \stackrel{k=N-1}{=} \\ &= \sum_{n=k}^{2k} \binom{n}{n-k} = \sum_{n=k}^{2k} \binom{n}{k}. \end{aligned}$$

Moreover, it is known that [17, p.160, Eq. 5.10] :

$$\sum_{i=0}^{n-1} \binom{i}{k} = \binom{n}{k+1}.$$

Thus, we have:

$$\begin{aligned} \sum_{n=k}^{2k} \binom{n}{k} &= \sum_{n=0}^{2k} \binom{n}{k} - \sum_{n=0}^{k-1} \binom{n}{k} = \binom{2k+1}{k+1} - \binom{k}{k+1} = \\ &= \binom{2k+1}{k+1} - 0 \stackrel{k=N-1}{=} \binom{2N-1}{N}. \end{aligned}$$

As a result, the sum term below is simplified to:

$$\sum_{n=0}^{N-1} \binom{N-1+n}{n} = \binom{2N-1}{N}. \quad (3.9)$$

Consequently, using Eqs. 3.7, 3.8, 3.9 the approximated average BER becomes:

$$P(e) \simeq \binom{2N-1}{N} \frac{1}{2^N} \left( \frac{1}{M^N \cdot \text{SNR}^N} \right) \in \mathcal{O} \left( \frac{1}{\text{SNR}^N} \right).$$

From asymptotic analysis above, a diversity order of  $N$  can be achieved.

### 3.3 Non-Coherent Detection

#### 3.3.1 ML non-coherent detector

The non-coherent detector must be independent of  $\tilde{\mathbf{h}}$ . For this reason, receiver design based on frequentist approach taking the expectation over  $\tilde{\mathbf{h}}$  of Eqs. 3.4, 3.5.

Thus,

$$f_{\mathbf{y}|H_0}(\mathbf{y} | H_0) = \mathbb{E}_{\tilde{\mathbf{h}}} [f_{\mathbf{z}|\mathbf{y},H_0}(\mathbf{z} | \mathbf{y}, H_0)], \quad (3.10)$$

$$f_{\mathbf{y}|H_1}(\mathbf{y} | H_1) = \mathbb{E}_{\tilde{\mathbf{h}}} [f_{\mathbf{z}|\mathbf{y},H_1}(\mathbf{z} | \mathbf{y}, H_1)]. \quad (3.11)$$

To proceed further, the following Lemma is needed:

**Lemma 3.** *For a Gaussian vector  $\mathbf{z} \sim \mathcal{CN}(\boldsymbol{\mu}, \boldsymbol{\Sigma})$  and a Hermitian matrix  $\mathbf{A}$ , the following identity holds true [18] :*

$$\mathbb{E} [\exp(-\mathbf{z}^\dagger \mathbf{A} \mathbf{z})] = \frac{\exp(-\boldsymbol{\mu}^\dagger \mathbf{A} (\mathbf{I} + \boldsymbol{\Sigma} \mathbf{A})^{-1} \boldsymbol{\mu})}{\det(\mathbf{I} + \boldsymbol{\Sigma} \mathbf{A})}.$$

□

The random vector  $\mathbf{z} = \mathbf{y} - \tilde{\mathbf{h}}x_i$ ,  $i \in \{0, 1\}$ , is defined with mean vector and covariance matrix, as follows:

$$\begin{aligned} \mathbb{E}_{\tilde{\mathbf{h}}} [\mathbf{z} | \mathbf{y}, H_i] &= \mathbb{E}_{\tilde{\mathbf{h}}} [\mathbf{y} - \tilde{\mathbf{h}}x_i | \mathbf{y}, H_i] = \mathbf{y}, \\ \mathbb{E}_{\tilde{\mathbf{h}}} [(\mathbf{z} - \mathbb{E}_{\tilde{\mathbf{h}}}[\mathbf{z}]) (\mathbf{z} - \mathbb{E}_{\tilde{\mathbf{h}}}[\mathbf{z}])^\dagger | \mathbf{y}, H_i] &= \mathbb{E}_{\tilde{\mathbf{h}}} [(\mathbf{z} - \mathbf{y}) (\mathbf{z} - \mathbf{y})^\dagger | \mathbf{y}, H_i] = \\ &= \mathbb{E}_{\tilde{\mathbf{h}}} [\tilde{\mathbf{h}} \tilde{\mathbf{h}}^\dagger | \mathbf{y}, H_i] x_i^2 = M x_i^2 \mathbf{I}_N, \end{aligned}$$

for  $i \in \{0, 1\}$ .

Applying Lemma 3 for  $\mathbf{A} = (\sigma^2 \mathbf{I}_N)^{-1}$ , Eqs. 3.10, 3.11 become:

$$\begin{aligned} f_{\mathbf{y}|H_0}(\mathbf{y} | H_0) &= \mathbb{E}_{\tilde{\mathbf{h}}} [f_{\mathbf{z}|\mathbf{y},H_0}(\mathbf{z} | \mathbf{y}, H_0)] \\ &= \frac{1}{(\pi\sigma^2)^N} \mathbb{E}_{\tilde{\mathbf{h}}} \left[ \exp \left( -\mathbf{z}^\dagger (\sigma^2 \mathbf{I}_N)^{-1} \mathbf{z} \right) | \mathbf{y}, H_0 \right] \\ &= \frac{1}{(\pi\sigma^2)^N} \exp \left( -\frac{\|\mathbf{y}\|_2^2}{\sigma^2} \right), \end{aligned}$$

$$\begin{aligned} f_{\mathbf{y}|H_1}(\mathbf{y} | H_1) &= \mathbb{E}_{\tilde{\mathbf{h}}} [f_{\mathbf{z}|\mathbf{y},H_1}(\mathbf{z} | \mathbf{y}, H_1)] \\ &= \frac{1}{(\pi\sigma^2)^N} \mathbb{E}_{\tilde{\mathbf{h}}} \left[ \exp \left( -\mathbf{z}^\dagger (\sigma^2 \mathbf{I}_N)^{-1} \mathbf{z} \right) | \mathbf{y}, H_1 \right] \\ &= \frac{1}{(\pi\sigma^2)^N} \frac{\exp \left[ -\mathbf{y}^\dagger \frac{1}{\sigma^2} \left( \left( \frac{Mx_1^2}{\sigma^2} + 1 \right) \mathbf{I}_N \right)^{-1} \mathbf{y} \right]}{\det \left[ \left( \frac{Mx_1^2}{\sigma^2} + 1 \right) \mathbf{I}_N \right]}. \end{aligned}$$

Applying MAP and assuming equiprobable symbols, we conclude to our ML non-coherent detector:

$$\begin{aligned} \hat{H}_i \text{ such that } i &= \arg \max_{j \in \{0,1\}} P(H_j | \mathbf{y}) \\ &= \arg \max_{j \in \{0,1\}} \frac{f_{\mathbf{y}|H_j}(\mathbf{y} | H_j) P(H_j)}{f_{\mathbf{y}}(\mathbf{y})} \\ &= \arg \max_{j \in \{0,1\}} f_{\mathbf{y}|H_j}(\mathbf{y} | H_j). \end{aligned}$$

After simple calculations, the ML non-coherent detector is simplified to:

$$f_{\mathbf{y}|H_1}(\mathbf{y} | H_1) \stackrel{H_1}{\geq} f_{\mathbf{y}|H_0}(\mathbf{y} | H_0) \Leftrightarrow$$

$$\frac{1}{(\pi\sigma^2)^N} \frac{\exp\left[-\mathbf{y}^\dagger \frac{1}{\sigma^2} \left(\left(\frac{Mx_1^2}{\sigma^2} + 1\right) \mathbf{I}_N\right)^{-1} \mathbf{y}\right]}{\det\left[\left(\frac{Mx_1^2}{\sigma^2} + 1\right) \mathbf{I}_N\right]} \stackrel{H_1}{\geq} \frac{1}{(\pi\sigma^2)^N} \exp\left(-\frac{\|\mathbf{y}\|_2^2}{\sigma^2}\right) \Leftrightarrow$$

$$\|\mathbf{y}\|_2^2 \stackrel{H_1}{\geq} \Theta, \quad (3.12)$$

where  $\Theta = N \frac{\sigma^2(1+2MSNR)}{2MSNR} \ln(1 + 2MSNR)$  and SNR is given by Eq. 2.2.

### 3.3.2 BER performance analysis

According to Eqs. 3.10, 3.11, the following statistics are available:

$$H_0 : \mathbf{y} = \mathbf{w} \sim \mathcal{CN}(\mathbf{0}_N, \sigma^2 \mathbf{I}_N),$$

$$H_1 : \mathbf{y} = \tilde{\mathbf{h}}x_1 + \mathbf{w} \sim \mathcal{CN}(\mathbf{0}_N, (Mx_1^2 + \sigma^2) \mathbf{I}_N).$$

Under  $H_0$ , the squared  $\mathcal{L}_2$  norm  $\|\mathbf{y}\|_2^2$  is distributed according to  $\sim \mathcal{G}(N, \sigma^2)$  and the conditional probability of error under  $H_0$  is given by:

$$\begin{aligned} P(e | H_0) &= P(\|\mathbf{y}\|_2^2 \geq \Theta | H_0) \\ &= P(x \geq \Theta | H_0) \\ &= \int_{\Theta}^{+\infty} \frac{1}{(\sigma^2)^N} \frac{1}{(N-1)!} x^{N-1} e^{-\frac{x}{\sigma^2}} dx \\ &= \frac{1}{(N-1)!} \int_{\frac{\Theta}{\sigma^2}}^{+\infty} y^{N-1} e^{-y} dy = \frac{1}{(N-1)!} \Gamma\left(N, \frac{\Theta}{\sigma^2}\right). \end{aligned}$$

Similarly, under  $H_1$ , the squared  $\mathcal{L}_2$  norm  $\|\mathbf{y}\|_2^2$  is distributed according to  $\sim \mathcal{G}(N, Mx_1^2 + \sigma^2)$  and the conditional probability of error under  $H_1$  is given by:

$$\begin{aligned}
P(e | H_1) &= P(\|\mathbf{y}\|_2^2 < \Theta | H_1) \\
&= P(x < \Theta | H_1) \\
&= \int_0^\Theta \frac{1}{(Mx_1^2 + \sigma^2)^N} \frac{1}{(N-1)!} x^{N-1} e^{-\frac{x}{Mx_1^2 + \sigma^2}} dx \\
&= \frac{1}{(N-1)!} \int_0^{\frac{\Theta}{Mx_1^2 + \sigma^2}} y^{N-1} e^{-y} dy = \frac{1}{(N-1)!} \gamma\left(N, \frac{\Theta}{Mx_1^2 + \sigma^2}\right).
\end{aligned}$$

Consequently, assuming equiprobable symbols, the average BER is:

$$P(e) = \frac{1}{2(N-1)!} \left[ \Gamma\left(N, \frac{\Theta}{\sigma^2}\right) + \gamma\left(N, \frac{\Theta}{\sigma^2(1 + 2(M \cdot \text{SNR}))}\right) \right], \quad (3.13)$$

where SNR is given by Eq. 2.2.

### 3.4 Single symbol case analysis

The case that only one phase is used ( $N=L=1$ ) is examined and the technique of interleaving or repetition coding is not deployed. This is the simplest way of beamforming, thus the system has no diversity and the BER performance is the worst. On the other hand no symbol transmission is repeated and no delay is included.

For  $N = L = 1$  the coherent and non-coherent detector is simplified to:

$$\Re\left(\frac{\tilde{h}_1^*}{|\tilde{h}_1|^2} y_1\right) \stackrel{H_1}{\geq} \frac{x_1}{2}$$

and

$$|y_1|^2 \stackrel{H_1}{\geq} \frac{\sigma^2(1 + 2MSNR)}{2MSNR} \ln(1 + 2MSNR) = \Theta,$$

where SNR is given by Eq. 2.2.

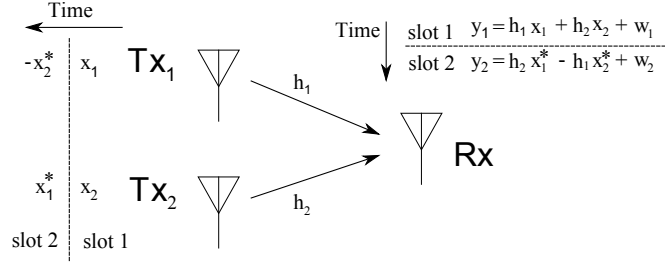


Figure 3.2: Alamouti reception scheme

Similarly, the BER formula for coherent and non-coherent case respectively is simplified to:

$$P(e) = \frac{1}{2} \left( 1 - \sqrt{\frac{M \cdot \text{SNR}}{2 + M \cdot \text{SNR}}} \right) \quad (3.14)$$

and

$$P(e) = \frac{1}{2} \left[ \left( e^{-\frac{\Theta}{\sigma^2}} \right) + \left( 1 - e^{-\frac{\Theta}{\sigma^2(1+2(M \cdot \text{SNR}))}} \right) \right], \quad (3.15)$$

where in Eq.(3.15) we use the properties  $\Gamma(1, t) = e^{-t}$  and  $\gamma(1, t) = 1 - e^{-t}$  to simplify the Eq.(3.13) for  $N = 1$ .

### 3.5 Alamouti reception scheme

For comparison purposes with single symbol case,  $2 \times 1$  Alamouti reception ( $M = 2$ ) is considered. B-PSK modulation ( $x_i = \pm\sqrt{E_s}$  for  $i = 0, 1$ ) and the same total transmission power per antenna terminal with single symbol case are assumed. The  $2 \times 1$  Alamouti reception transmits 2 symbols in 2 slots (Fig. 3.2) and achieves a diversity order of 2, thus the total transmit power per antenna terminal is given by:

$$\mathbb{E} [ |x|^2 ]_{\text{Alamouti}}^{\text{total}} = \mathbb{E} [ |x_1|^2 ]_{\text{Alamouti}}^{\text{slot 1}} + \mathbb{E} [ |x_2|^2 ]_{\text{Alamouti}}^{\text{slot 2}} = E_s + E_s = 2E_s.$$

For the single symbol distributed beamforming case with OOK, the total transmission power per antenna terminal per slot is given by:

$$\mathbb{E} [|x|^2]_{\text{OOK}}^{\text{total}} = E_1/2.$$

Thus,

$$E_s = E_1/4. \quad (3.16)$$

The SNR for Alamouti reception is defined as:

$$\text{SNR}_{\text{Alamouti}} = \frac{\mathbb{E} [|x_1|^2]_{\text{Alamouti}}}{\mathbb{E} [|w|^2]} = \frac{\mathbb{E} [|x_2|^2]_{\text{Alamouti}}}{\mathbb{E} [|w|^2]} = \frac{E_s}{\sigma^2} \stackrel{3.16}{=} \frac{E_1}{4\sigma^2} = \frac{\text{SNR}}{2},$$

where SNR is defined in Eq. 2.2. As a result BER for  $2 \times 1$  Alamouti reception using Eq. [16, p.62, Eq. 3.37] is given by:

$$P(e) = \left( \frac{1 - \mu}{2} \right)^2 \cdot (2 + \mu),$$

where  $\mu = \sqrt{\frac{\text{SNR}_{\text{Alamouti}}}{1 + \text{SNR}_{\text{Alamouti}}}} = \sqrt{\frac{\text{SNR}}{2 + \text{SNR}}}$  and SNR is given by Eq. 2.2.

## 3.6 Simulation

Similarly to repetition coding protocol, the numerical results assume  $f_c = 2.4$  GHz,  $T_s = 1 \mu s$  and 20 ppm clock crystals. For single symbol and interleaving distributed beamforming transmission, the same total transmission power per antenna terminal is assumed, thus:

$$\frac{E_1^s}{2\sigma^2} = \frac{NE_1^i}{2\sigma^2} \triangleq \text{SNR per transmitter antenna},$$

where  $E_1^s, E_1^i$  denote the transmission power of symbol  $x_1$  for single symbol and repetition coding distributed beamforming transmission respectively. Under the assumption of the same total transmission power per antenna terminal, performance comparison is meaningful for the different systems.

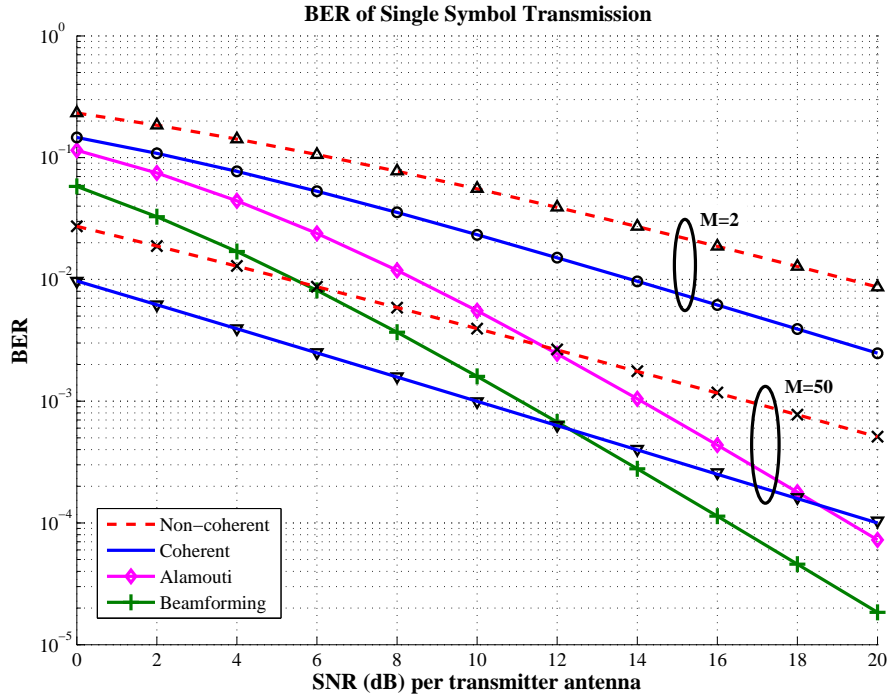


Figure 3.3: Simulation and analysis BER performance for symbol case with different number of transmitters

Fig. 3.3 depicts BER performance for a single phase ( $N = 1$ ), where it is noticeable that as the number of transmitters  $M$  is increased, BER is improved even at low SNR at the expense of total transmission power. For comparison reasons, Alamouti  $2 \times 1$  reception and coherent transmit beamforming schemes are also depicted, assuming the same total transmission power with our setup for both of them. The two aforementioned systems differ in 3 dB in terms of BER performance and offer second order diversity. For a large number of transmitters ( $M = 50$ ), it can be interestingly seen that non-coherent distributed beamforming reception achieves substantial performance at low SNR compared to the other schemes, at the expense of total transmission power. Interleaving protocol exploits diversity due to the independent channel realizations (phases) at the expense of reception delay. Fig. 3.4 depicts BER performance for different number of phases. As number of phases is increased, BER drops faster for high SNR due to channel diversity. For com-

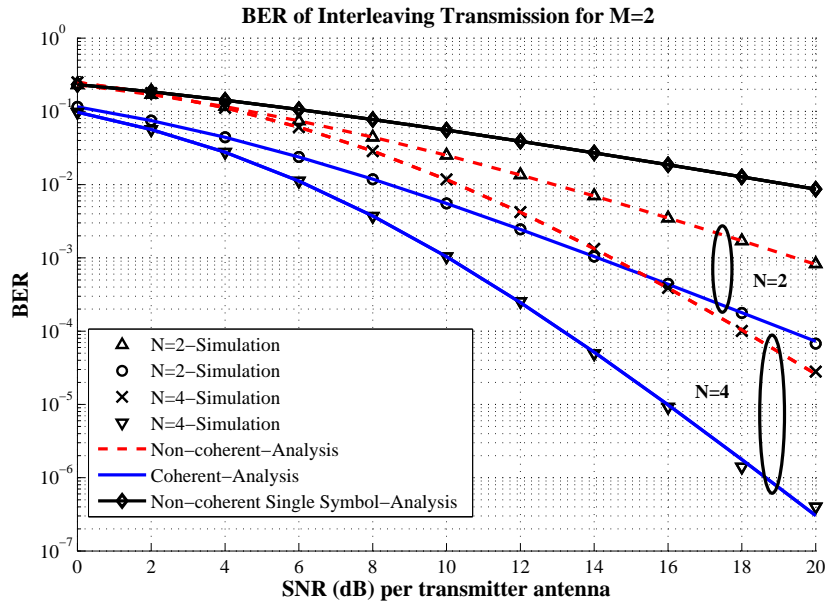


Figure 3.4: Simulation and analysis BER performance for interleaving transmission in different phases

pleteness, BER for ML coherent detectors is depicted for both single symbol and interleaving distributed transmission. On the other hand, interleaving protocol can be further improved exploiting the beamforming gains. Fig. 3.5 shows for fixed  $N = 2$  that BER improvement can be achieved at low SNR by increasing the number  $M$  of transmitters. Finally, all the experimental result via Monte Carlo simulations match our analytic study very well.

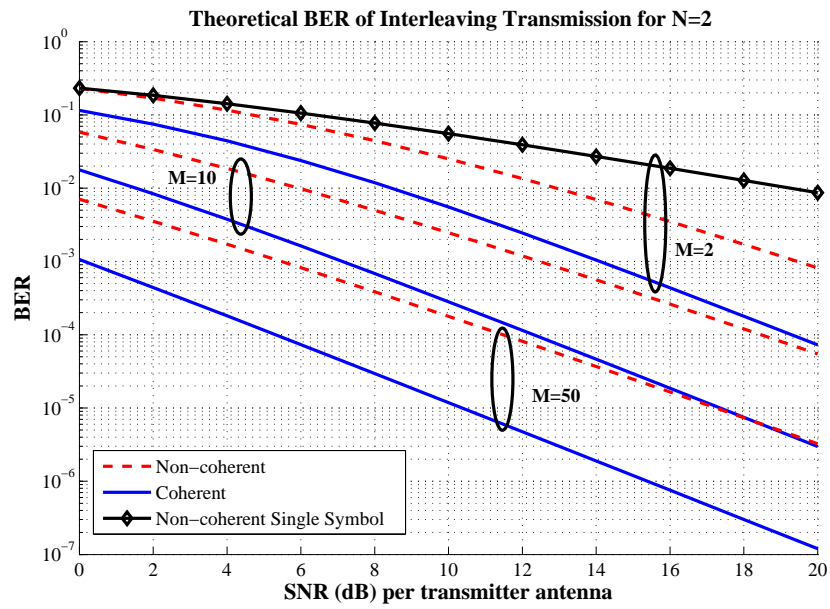


Figure 3.5: Simulation and analysis BER performance for interleaving transmission with different number of transmitters



## Chapter 4

# Unitary Space-Time Constellations

In this chapter a brief note on constellations of unitary space-time signals is provided. The information-theoretic capacity-related results for centralized multi-input multi-output (MIMO) non-coherent reception in [19], suggest a signal structure through unitary space-time signals [20]. Unitary space-time signals, which are orthonormal in time across the antennas, offer acceptable performance by exploiting multiple-antenna diversity. For completeness, we apply unitary space-time modulation (USTM) in our distributed model and demonstrate its BER performance in comparison with the centralized case in [21].

### 4.1 System model

A non-coherent detector for a centralized MIMO system with unitary space-time modulation is presented in [21]. The system considers  $M$  transmitting antennas and  $N$  receiving antennas. Furthermore, no CFO parameters are incorporated, since the transmitters are not distributed. The Rayleigh, flat fading coefficients between transmitting and receiving antennas remain constant for  $T$  symbols and the model is given by:

$$\mathbf{Y} = \sqrt{\frac{\rho}{M}} \mathbf{S} \mathbf{H} + \mathbf{W}, \quad (4.1)$$

where  $\mathbf{Y}$  is the  $T \times N$  complex matrix of the received signals,  $\mathbf{S}$  is the  $T \times M$  space-time coding matrix of the transmitted signals,  $\mathbf{H}$  is the  $M \times N$  matrix of Rayleigh fading coefficients,  $\mathbf{W}$  is the  $T \times N$  matrix of additive

CWGN receiver noise and  $\rho$  represents the expected SNR at each receiving antenna per time slot. Taking into account the MISO special case of MIMO design described in Eq. 4.1 and introducing CFO parameters by extending the centralized case for a single receiver, the model simplifies to a  $T \times 1$   $\tilde{\mathbf{y}}$  vector, where its  $t^{\text{th}}$  element is given by:

$$\tilde{y}_t = \sqrt{\frac{\rho}{M}} \sum_{m=1}^M h_m e^{j2\pi\Delta f_m t T_s} s_{tm} + w_t, \quad (4.2)$$

$t \in \{1, \dots, T\}$ .

## 4.2 Non-coherent detector

In [19], [20] has been shown that the capacity-achieving distribution for  $T \gg M$  and for a fixed  $\rho$  is  $\mathbf{S} = \sqrt{T}\mathbf{\Phi}$ , where  $\mathbf{\Phi}^\dagger \mathbf{\Phi} = \mathbf{I}_M$  and  $\mathbf{\Phi}$  is isotropically distributed. For details about the isotropic distribution, the interested reader could refer to [19]. A defining characteristic of isotropic distribution is that  $\mathbf{\Phi}$  and  $\mathbf{\Theta}\mathbf{\Phi}$  have the same distribution for any deterministic unitary  $\mathbf{\Theta}$ . Considering constellation of  $L = 2^{R \times T}$  signals ( $\mathbf{S}_1 = \sqrt{T}\mathbf{\Phi}_1, \dots, \mathbf{S}_L = \sqrt{T}\mathbf{\Phi}_L$ ), with  $R$  denotes the bit/symbol rate, the maximum likelihood decoder for a constellation of unitary space-time signals is given by [21, Eq. 3]:

$$\mathbf{\Phi}_{\text{ML}} = \arg \max_{\mathbf{\Phi}_1, \dots, \mathbf{\Phi}_L} \text{tr} \left\{ \mathbf{Y}^\dagger \mathbf{\Phi}_l \mathbf{\Phi}_l^\dagger \mathbf{Y} \right\}, \quad (4.3)$$

where  $l \in \{1, \dots, L\}$ . The model defined in Eq. 4.2 is assumed and the detector above is applied. Thus, we result in the following sub-optimal detector:

$$\hat{\mathbf{\Phi}} = \arg \max_{\mathbf{\Phi}_1, \dots, \mathbf{\Phi}_L} \text{tr} \left\{ \tilde{\mathbf{y}}^\dagger \mathbf{\Phi}_l \mathbf{\Phi}_l^\dagger \tilde{\mathbf{y}} \right\}. \quad (4.4)$$

### 4.3 Systematic design of unitary space-time constellations

The main idea behind the design of a unitary space-time constellation is the probability of error minimization. Specifically, for the model described by Eq. 4.1, it is unable to compute the block probability of error  $P_e$  for a general constellation of unitary space-time signals. On the other hand, the performance can be upper-bounded in terms of pairwise error probabilities (PEP) through the union and Chernoff bound and is given by [21, Eq. 12]:

$$\begin{aligned}
 P_e &\leq \frac{1}{L} \sum_{l=1}^L \sum_{l' \neq l} \frac{1}{2} \left[ \frac{1}{1 + \frac{(\rho T/M)^2}{4(1+\rho T/M)}} \right]^{N \cdot (M - \lceil M \|\Phi_l^\dagger \Phi_{l'}\|^2 \rceil)} \\
 &\leq \frac{1}{2} \left[ \frac{1}{1 + \frac{(\rho T/M)^2}{4(1+\rho T/M)}} \right]^{N \cdot (M - \lceil M \delta^2 \rceil)}, \tag{4.5}
 \end{aligned}$$

where  $\delta = \max_{1 \leq l < l' \leq L} \|\Phi_l^\dagger \Phi_{l'}\|$ . For achieving probability of error upper-bound minimization, constellations that minimize  $\delta$  must be constructed. In [21], two basic systematic ways of constellations construction are proposed. The first one is a Fourier based construction and the second one is an equivalent algebraic construction. In this subsection, only the equivalent algebraic construction is presented.

Let  $R_q = \{0, \dots, q-1\}$  and  $\mathbf{l} = [l_1, \dots, l_K]^T$  be a  $K \times 1$  vector, where  $l_k \in R_q, \forall k \in \{1, \dots, K\}$ , thus the size of the constellation is  $L = q^K = 2^{R \times T}$ . Given  $\mathbf{U}$ , a systematic generator matrix of the form:

$$\mathbf{U} = [\mathbf{I}_K \ \mathbf{U}'],$$

where  $\mathbf{I}_K$  is the  $K \times K$  identity matrix and  $\mathbf{U}'$  is a  $K \times (T - K)$  parity matrix with elements in  $R_q$ , the  $\Phi_l$  matrix of the unitary space-time signal

$\mathbf{S}_l$  of constellation size  $L$  can be determined as:

$$\mathbf{\Phi}_l = \mathbf{\Theta}_1^{l_1} \cdot \mathbf{\Theta}_2^{l_2} \cdot \dots \cdot \mathbf{\Theta}_K^{l_K} \cdot \mathbf{\Phi}_1, \quad l \neq 1$$

such that  $\delta_{\min} = \min_{\mathbf{U}'} \max_l \sqrt{\frac{1}{M}} \|\mathbf{\Phi}_l^\dagger \mathbf{\Phi}_{l'}\|,$

where  $\mathbf{\Theta}_1, \mathbf{\Theta}_2, \dots, \mathbf{\Theta}_K$  diagonal  $T \times T$  complex matrices with entries  $[\mathbf{\Theta}_k]_{tt} = \phi(\mathbf{U}_{kt})$ ,  $k \in \{1, \dots, K\}$ ,  $t \in \{1, \dots, T\}$ .

The function  $\phi(\mathbf{x}) = \frac{1}{\sqrt{T}} \left[ e^{j\frac{2\pi}{q}x_1} \ e^{j\frac{2\pi}{q}x_2} \ \dots \ e^{j\frac{2\pi}{q}x_T} \right]^T$ ,  $\mathbf{x} \in \mathbb{N}^T$  and  $\mathbf{\Phi}_1$  a  $T \times M$  DFT matrix. The minimization of  $\delta$  parameter implies minimization of maximum correlation of subspaces of  $\mathbb{C}^T$  spanned by columns of  $\mathbf{\Phi}_l$  and  $\mathbf{\Phi}_{l'}$ . Thus, the proposed algebraic construction of constellations searches for minimization of their correlation. According to [21, Theorem 1], all the unitary space-time signals can be expressed as a function of  $\mathbf{\Phi}_1$ , as a result the term  $\|\mathbf{\Phi}_l^\dagger \mathbf{\Phi}_{l'}\|$  is simplified to  $\|\mathbf{\Phi}_1^\dagger \mathbf{\Phi}_{l'}\|$  and only  $L - 1$  iterations are required to find maximum correlation of constellations for a given  $\mathbf{U}'$ .

## 4.4 Simulation

Fig. 4.1 depicts BER performance of USTM, for the cases with and without CFO's; constellation of  $2^{R \times T}$  signals was assumed, with  $R = 1$  bit/symbol and  $T = 8$ . The unitary space time signals were constructed for  $M = 2$  transmitting antennas,  $K = 1$ ,  $q = 257$  ([21, Table I]). Without CFO's, USTM achieves reduced BER, while for the distributed case (i.e. presence of  $\{\Delta f_m\}$ ), performance is degraded, as expected, since USTM has been designed for the centralized MIMO case. Consequently, new different distributed schemes need to be considered for the case of USTM in presence of CFOs.

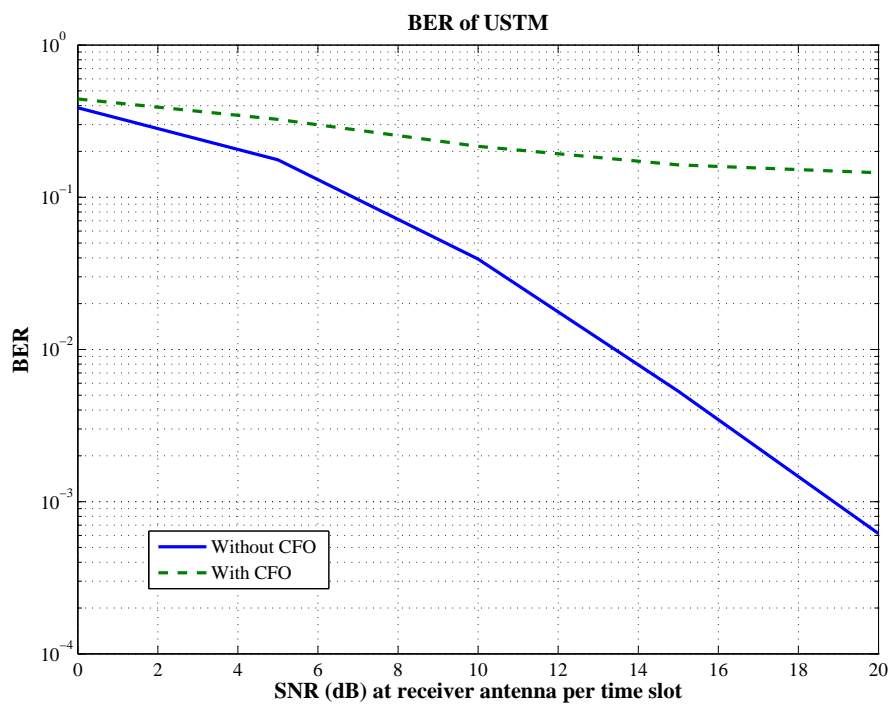


Figure 4.1: Simulation BER performance using USTM for  $M = 2$ ,  $T = 8$  and  $R = 1$  bit/symbol



# Chapter 5

## Conclusions and future work

### 5.1 Conclusions

Distributed zero-feedback (i.e. blind) constructive signal alignment is feasible and can be exploited in resource-constrained networks to provide up to  $M^2$ -fold power gain with  $M$  collaborating transmitters. Two concrete non-coherent receivers were proposed to enhance communication link reliability in terms of BER performance.

A heuristic, near-optimal receiver, based on repetition coding, showed that repetitive transmission takes advantage of probabilistic alignment and provides constructive beamforming gain. Another scheme based on interleaving was presented and provided diversity benefits at the expense of additional delay. BER performance for the aforementioned setups proposed was evaluated via simulations and analytical results.

Finally, and for completeness, USTM was evaluated in the context of our distributed MISO model and its BER was evaluated, showing that USTM designs need to be revised for the distributed case.

### 5.2 Future work

For the case of USTM, simulation results showed that new different distributed schemes need to be considered for CFOs' presence as future work. Moreover, following the analysis and the numerical results in this thesis, it can be easily seen that the proposed beamforming schemes could be easily implemented using commodity, off-the-self radios. Initial implementation results that offer experimental validation using low-cost commodity radio hardware are underway [22–24].



# Appendix A

## A.1 Proper complex Gaussian random vectors

A definition and a theorem for proper complex Gaussian random vectors are presented below:

**Definition 1.** A complex random vector  $\mathbf{v} = \mathbf{v}_R + j\mathbf{v}_I$  will be called proper if its pseudocovariance vanishes, i.e.,  $\mathbf{M}_{\mathbf{v}} = \mathbb{E} \left[ (\mathbf{v} - \mathbb{E}[\mathbf{v}]) (\mathbf{v} - \mathbb{E}[\mathbf{v}])^T \right] = \mathbf{O}_n$ .

**Theorem 2.** Let  $\mathbf{x}$  be a proper complex  $N$ -dimensional Gaussian random vector with mean  $\boldsymbol{\mu}_{\mathbf{x}}$  and nonsingular covariance matrix  $\boldsymbol{\Sigma}_{\mathbf{x}}$ . Then the pdf of  $\mathbf{x}$  is given by [15]:

$$f_{\mathbf{x}}(\mathbf{x}) = \frac{1}{\pi^N \det(\boldsymbol{\Sigma}_{\mathbf{x}})} \exp \left\{ -(\mathbf{x} - \boldsymbol{\mu}_{\mathbf{x}})^\dagger \boldsymbol{\Sigma}_{\mathbf{x}}^{-1} (\mathbf{x} - \boldsymbol{\mu}_{\mathbf{x}}) \right\}.$$

## A.2 Gamma distribution

A random variable  $X$  is Gamma distributed, iff its pdf is given by:

$$f_X(x; k, \theta) = \frac{1}{\theta^k} \cdot \frac{1}{\Gamma(k)} \cdot x^{k-1} \cdot e^{-\frac{x}{\theta}} \cdot u(x),$$

where  $u(\cdot)$  denotes the step function and  $\Gamma(k) = (k-1)!$  for any positive integer.



# Bibliography

- [1] N. D. Sidiropoulos, T. N. Davidson, and Z. Q. Luo, “Transmit beamforming for physical layer multicasting,” *IEEE Trans. Signal Processing*, vol. 54, no. 6, pp. 2239–2251, Jun. 2006.
- [2] V. H. Nassab, S. Shahbazpanahi, A. Grami, and Z. Q. Luo, “Distributed beamforming for relay networks based on second-order statistics of the channel state information,” *IEEE Trans. Signal Processing*, vol. 56, no. 9, pp. 4306–4316, Sep. 2008.
- [3] S. Song, J. Thompson, P.-J. Chung, and P. Grant, “BER Analysis for Distributed Beamforming With Phase Errors,” *Vehicular Technology, IEEE Transactions on*, vol. 59, no. 8, pp. 4169–4174, Oct. 2010.
- [4] R. Mudumbai, B. Wild, U. Madhow, and K. Ramchandran, “Distributed beamforming using 1 bit feedback: from concept to realization,” in *Proc. Allerton Conf. on Communication, Control and Computing*, Sep. 2006, pp. 1020–1027.
- [5] M. Johnson, K. Ramchandran, and M. Mitzenmacher, “Distributed beamforming with binary signaling,” in *Proc. IEEE Int. Symp. on Inform. Theory*, Jul. 2008, pp. 890–894.
- [6] R. Mudumbai, D. R. Brown, U. Madhow, and H. V. Poor, “Distributed transmit beamforming: Challenges and recent progress,” *IEEE Commun. Mag.*, vol. 47, no. 2, pp. 102–110, Feb. 2009.
- [7] R. Mudumbai, G. Barriac, and U. Madhow, “On the feasibility of distributed beamforming in wireless networks,” *IEEE Trans. Wireless Commun.*, vol. 6, no. 5, pp. 1754–1763, May 2007.

- 
- [8] J. Uher, T. Wysocki, and B. Wysocki, “Review of distributed beamforming,” *Journal of Telecommunications and Information Technology*, 2011.
- [9] Y. Lebrun, K. Zhao, S. Pollin, A. Bourdoux, F. Horlin, and R. Lauwereins, “Performance analysis of distributed zf beamforming in the presence of cfo,” *EURASIP Journal on Wireless Communications and Networking*, Nov 2011.
- [10] A. Bletsas, A. Lippman, and J. Sahalos, “Simple, zero-feedback, distributed beamforming with unsynchronized carriers,” *IEEE J. Select. Areas Commun.*, vol. 28, no. 7, pp. 1046–1054, Sep. 2010.
- [11] —, “Zero-feedback, collaborative beamforming for emergency radio: Asymptotic analysis,” *Mobile Networks and Applications (MONET)*, vol. 16, no. 5, pp. 589–599, Oct. 2011.
- [12] M. S. Alouini, A. Abdi, and M. Kaveh, “Sum of gamma variates and performance of wireless communication systems over nakagami-fading channels,” *IEEE Trans. Veh. Technol.*, vol. 50, no. 6, pp. 1471–1479, 1993.
- [13] J. F. Paris, “A note on the sum of correlated gamma random variables,” Mar. 2011, arXiv:1103.0505.
- [14] M. Abramowitz and I. A. Stegun, *Handbook of Mathematical Functions with Formulas, Graphs, and Mathematical Tables*. New York: Dover, 1964.
- [15] F. Nesser and J. Massey, “Proper complex random processes with applications to information theory,” *IEEE Trans. Inform. Theory*, vol. 39, no. 7, pp. 1293–1302, Jul. 1993.
- [16] D. Tse and P. Viswanath, *Fundamentals of Wireless Communications*. Cambridge University Press, 2005.
- [17] R. Graham, D. Knuth, and O. Patashnik, *Concrete Mathematics: A Foundation for Computer Science*. Addison-Wesley, 1994.

- 
- [18] S. Zhou and G. B. Giannakis, "MIMO communications with partial channel state information," in *Space Time Processing for MIMO Communications* (eds A. B. Gershman and N. D. Sidiropoulos). John Wiley & Sons, 2005, pp. 319–355.
- [19] T. L. Marzetta and B. M. Hochwald, "Capacity of a mobile multiple-antenna communication link in rayleigh flat fading," *IEEE Trans. Inform. Theory*, vol. 45, pp. 139–157, Jan. 1993.
- [20] B. M. Hochwald and T. L. Marzetta, "Unitary space-time modulation for multiple-antenna communication in rayleigh flat-fading," *IEEE Trans. Inform. Theory*, vol. 46, pp. 543–564, Mar. 2000.
- [21] B. Hochwald, T. Marzetta, T. Richardson, W. Sweldens, and R. Urbanke, "Systematic design of unitary space-time constellations," *IEEE Trans. Inform. Theory*, vol. 46, no. 6, pp. 1962–1973, Sep. 2000.
- [22] K. Alexandris, G. Sklivanitis, and A. Bletsas, "Non-coherent receivers for zero-feedback distributed beamforming," under preparation.
- [23] G. Sklivanitis and A. Bletsas, "Testing zero-feedback distributed beamforming with a low-cost SDR testbed," in *Signals, Systems and Computers (ASILOMAR), 2011 Conference Record of the Forty Fifth Asilomar Conference on*, Nov. 2011, pp. 104–108.
- [24] G. Sklivanitis, "Disruptive communications," Master's thesis, ECE Department, Technical University of Crete, Chania, Greece, under preparation.